

# How to detect fluctuating order in the high-temperature superconductors

S. A. Kivelson,<sup>1</sup> E. Fradkin,<sup>2</sup> V. Oganesyan,<sup>3</sup> I. P. Bindloss,<sup>1</sup> J. M. Tranquada,<sup>4</sup> A. Kapitulnik,<sup>5</sup> and C. Howald<sup>5</sup>  
<sup>1</sup>Department of Physics, University of California at Los Angeles, 405 Hilgard Ave. , Los Angeles, CA 90095  
<sup>2</sup>Department of Physics, University of Illinois, 1110 W. Green St. , Urbana IL 61801-3080  
<sup>3</sup>Department of Physics, Princeton University, Princeton NJ 08544  
<sup>4</sup>Brookhaven National Laboratory, Upton, New York 11973-5000  
<sup>5</sup>Department of Physics, Stanford University, Stanford, CA 94305-4045

(Dated: May 21, 2019)

We discuss fluctuating order in a quantum disordered phase proximate to a quantum critical point, with particular emphasis on fluctuating stripe order. Optimal strategies for deriving information concerning such local order from experiments are derived with emphasis on neutron scattering and scanning tunnelling microscopy. These ideas are applied to two model systems - the exactly solvable one dimensional electron gas with an impurity, and a weakly interacting 2D electron gas. Finally, we extensively review experiments on the cuprate high temperature superconductors which can be analyzed using these strategies. We adduce evidence that stripe correlations are widespread in the cuprates.

## Contents

<b>I. Introduction</b>	1
<b>II. General Considerations</b>	2
A. Stripe ordered phases	2
B. Fluctuating order near a quantum critical point	3
C. How weak disorder can make life simpler	4
D. Response functions	4
E. Phase diagrams	5
<b>III. One-dimensional Luttinger Liquid</b>	6
<b>IV. Two-dimensional Fermi Liquid</b>	9
<b>V. Regarding experiments in the cuprates</b>	11
A. Diffraction from stripes	12
B. STM measurements and stripes	13
1. Concerning differing interpretations of the STM spectra	14
C. Detecting Nematic Order	15
1. Transport Anisotropies	15
2. Anisotropic Diffraction Patterns	16
3. STM Imaging of Nematic Order	17
D. “1/8” Anomaly	17
E. Other Probes	18
<b>VI. Conclusions</b>	20
<b>VII. Acknowledgments</b>	20
<b>Note Added:</b>	21
<b>References</b>	21

## I. INTRODUCTION

Ordered states of matter are characterized by a broken symmetry. Depending on various real-world details, this may be relatively easier or harder to detect experimentally, but once detected it is unambiguous. The notion that order parameter fluctuations are important in the disordered phase proximate to an ordered state is a rather obvious extension of the idea of broken symmetry. However, this notion is more difficult to define precisely,

much less to detect experimentally. To develop this important notion, we will discuss strategies for detecting quantum fluctuating stripe order in the putative stripe liquid phase of the high temperature superconductors (1). More generally, we are interested in electronic liquid crystalline states and their associated fluctuations,(5) but the results are also easily generalized to other forms of order (6).

Since the whole notion of fluctuating order is based on proximity of an ordered state, it is essential first to establish the existence of the “nearby” ordered state by directly detecting the relevant broken symmetry. The ordered phase may be induced by making small changes to the chemical composition of the material, applying pressure or magnetic fields, etc. Unless an actual ordered state can be reached, it is dangerous to speculate about the effects of related fluctuating order.

Typically, the best way to detect both the broken symmetry state and the relevant fluctuations is by measuring the appropriate dynamical structure factor,  $S(\mathbf{q}, \omega)$ . Indeed, X-ray and neutron scattering studies have provided the best evidence (1; 12) of ordered and fluctuating stripe phases, as we shall discuss. However, in many interesting materials, appropriate crystals are not available and so such experiments are not possible. Here, probes of local order, such as nuclear magnetic resonance (NMR), nuclear quadrupole resonance (NQR), muon spin rotation ( $\mu$ SR), and scanning tunneling microscopy (STM) techniques, may be the best available. All of these are quasi-static (*i.e.*, nearly zero frequency) probes. In a pure quantum system, in its disordered phase, the order-parameter fluctuations are typically gapped, with a characteristic gap frequency that grows with the distance  $\ell$  to the quantum critical point. Thus, unless something is done to “pin” these fluctuations, they are invisible to these local probes. Such pinning is induced by boundaries, vortices, crystal-field effects, weak quenched disorder, etc. This is uniquely a problem associated with quantum fluctuations, and does not have an analogue in

classical critical phenomena.

**In this article**, we first discuss results obtained for solvable model systems, which we analyze in various ways to illustrate the optimal strategies for extracting information about local order. In particular, much of this discussion addresses the character of the local order in a quantum disordered phase close to a quantum critical point; we believe that the intuitions gleaned from this study are more generally valid, but without the nearness to the critical point as a small parameter, it is difficult to treat the more general problem in a controlled fashion. We also review in some depth, although by no means exhaustively, the experimental evidence of various forms of stripe order in the cuprate superconductors. There are several related topics that we do not cover in this article; instead, we direct the interested reader to recent reviews. Specifically, the mechanism of stripe formation(15) is not discussed at all, and the possible relevance(24) of local stripe order to the mechanism of high temperature superconductivity and to the various remarkable normal state properties observed in the cuprates is only touched on briefly. The present paper should, in our opinion, be considered in the context of the broader issue of the role of “competing orders” in the high temperature superconductors.(28) The reader may also want to refer to other recent reviews of the evidence of stripes in the cuprates, of which some recent ones are listed in Ref. (34).

In Section II we discuss basic scaling considerations that govern the relevant length, frequency, and energy scales of fluctuating order in the neighborhood of a quantum critical point, and the consequences of the pinning induced by disorder and other perturbations. We show that it is the low frequency part of the dynamical structure factor, rather than its integral over all frequencies, that contains the clearest information concerning local order. We also define a new response function which determines the local density-of-states modulations induced by a weak impurity potential. Finally, we sketch various possible versions of the phase diagram of a system with competing stripe and superconducting phases, to illustrate how the various considerations apply in different circumstances.

In Section III, we consider a theoretically well understood system, the one dimensional electron gas (1DEG) in the presence of an impurity. We compute the local density of states (as would be measured in STM) and the dynamical structure factor, and show by this explicit example how the general considerations articulated in the present paper are manifest in this solvable model. (The 1DEG can also be viewed as a quantum critical state associated with CDW order.) In addition to its pedagogical value, this section contains explicit results that should be useful for analyzing STM experiments on quasi 1D systems with dilute impurities, such as (35) the chain-layers of YBCO, or STM experiments on carbon nanotubes(36). In Section IV we repeat the DOS calculation in the context of a simple system with quasi-particles: the weakly interacting electron gas in two dimensions.

In Section V we discuss applications of these ideas to experiments in the cuprates; in Section V.A we discuss diffraction studies, and in Section V.B STM studies. This latter section contains new insights concerning the optimal way to analyze STM data to extract information about fluctuating order; applying these ideas to the recent experimental results of Hoffman *et al.* (37; 38), and Howald *et al.* (39), clearly reveals the existence of a nearby stripe ordered phase in optimally doped BSCCO. (This conclusion is in agreement with the inferences drawn from the data by Howald *et al.*, but in disagreement with the inferences drawn by Hoffman *et al.*; we will discuss the origins of the differing conclusions.) Section V.C contains a discussion of experiments to detect local nematic order, and a discussion of recent STM evidence of such order on the same BSCCO surfaces. In Section V.D, we discuss indirect evidence of stripe order that comes from the “1/8 anomaly.” Throughout the paper, our most important conclusions are embodied in five numbered “Lessons,” which are summarized in Section VI.

## II. GENERAL CONSIDERATIONS

### A. Stripe ordered phases

“Stripes” is a term that is used to describe unidirectional density wave states, which can involve unidirectional charge modulations (“charge stripes”) or coexisting charge and spin density order (“spin stripes”).(40) In 2D, an ordered stripe phase with the stripes running in the  $y$  direction gives rise to new Bragg peaks in the electron charge density (and corresponding peaks in the nuclear density) at  $\mathbf{k} = \pm\mathbf{k}_{ch} = \pm\delta_{ch}\hat{e}_x$  and harmonics, where  $\delta_{ch} = 2\pi/\lambda_{ch}$  and  $\lambda_{ch}$  is the charge stripe period. Where spin order coexists with charge order, new magnetic Bragg peaks occur at harmonics of  $\mathbf{k} = \mathbf{k}_s = \pi \pm (1/2)\mathbf{k}_{ch}$  where  $\pi = \pi[\hat{e}_x + \hat{e}_y]$  is the Néel ordering vector. (Note, in a crystal, wave vector equalities are always to be interpreted as meaning equal up to a reciprocal lattice vector.)

Charge stripes break rotational symmetry and translation symmetry perpendicular to the stripes—in a crystal, these are to be interpreted as breaking of the crystal symmetry group, rather than the continuous symmetries of free space. The relevant order parameter,  $\langle \rho_{\mathbf{k}_{ch}} \rangle$ , is the Fourier component of the electron charge density at the ordering wave vector. If the state is, in addition, a conducting or superconducting electron fluid, it is a charge stripe smectic. Spin stripes, in addition, break spin-rotational and time reversal invariance (although a particular combination of time reversal and translation is preserved). Wherever there is spin stripe order, there is necessarily (42) charge stripe order, as well. The new order parameter which distinguishes the spin stripe phase,  $\langle \mathbf{s}_{\mathbf{k}_s} \rangle$ , is the Fourier component of the spin-density.

There is more than one possible stripe liquid phase. In

particular, there is the possibility of a “stripe nematic” phase, in which thermal or quantum fluctuations have caused the stripe ordered state to melt (*i.e.*, translational symmetry is restored) but orientational symmetry remains broken (*i.e.* a snapshot of the system is more likely to see stripe segments oriented in the  $y$  than  $x$  direction). This state shares with a stripe-ordered state a precise definition in terms of broken symmetry. The order parameter can be taken to be any physical quantity transforming like a traceless symmetric tensor. For instance, the traceless part of the dielectric tensor is a measure of nematic order of the charge fluid. In two dimensions, a useful nematic order parameter is also

$$\mathcal{Q}_{\mathbf{k}} \equiv \frac{S(\mathbf{k}) - S(\mathcal{R}[\mathbf{k}])}{S(\mathbf{k}) + S(\mathcal{R}[\mathbf{k}])}, \quad (2.1)$$

where  $\mathcal{R}$  is a rotation by  $\pi/2$ , and

$$S(\mathbf{k}) = \int_{-\infty}^{\infty} \frac{d\omega}{2\pi} S(\mathbf{k}, \omega) \quad (2.2)$$

is the thermodynamic (equal time) structure factor. More exotic states can also occur, such as a “nematic spin-nematic,” which breaks rotational, spin rotational, and time reversal symmetry, but not the product of  $\mathcal{R}$  and time reversal(43).

## B. Fluctuating order near a quantum critical point

We consider a system in a quantum disordered phase near to a quantum critical point beyond which the ground state would be ordered (44; 45). To be concrete, we will discuss charge stripe order, but the considerations have more general validity. By the quantum disordered phase, we mean one in which there is no long-range stripe order as  $T \rightarrow 0$ , but there may be other forms of order, for instance superconducting order, so long as we are nowhere near the quantum critical point for this other order.

The charge-density dynamical structure factor,  $S_{\text{ch}}(\mathbf{k}, \omega)$ , for  $\mathbf{k}$  in the neighborhood of  $\mathbf{k}_{\text{ch}}$ , measures the collective fluctuations which are most sensitive to the proximity of the quantum critical point. The scaling theory of quantum critical phenomena tells us that, on the quantum disordered side of the quantum critical point, there are diverging length and time scales,  $\xi \sim \ell^{-\nu}$  and  $\tau \sim \ell^{-\nu z}$  where  $\nu$  is a critical exponent,  $z$  is the dynamical critical exponent, and  $\ell$  is a dimensionless measure of the distance to the quantum critical point(46).

In the quantum disordered phase, and in the absence of quenched disorder, the fluctuation spectrum typically (47) has a gap, which we will denote by  $E_{\text{G}}$ , related to the correlation time by the scaling law  $E_{\text{G}} \sim \hbar/\tau \sim \ell^{\nu z}$ . For  $\hbar\omega$  slightly larger than  $E_{\text{G}}$ ,  $S(\mathbf{k}, \omega)$  has a pole corresponding to a sharply defined elementary excitation; this “soft-mode” is the quantity which condenses across

the quantum critical point, so its quantum numbers and characteristic wave vector directly encode the nature of the nearby ordered state. At somewhat higher energy (typically, for  $\hbar\omega > 3E_{\text{G}}$ )  $S(\mathbf{k}, \omega)$  exhibits a multi-particle continuum. Deep in the continuum the system effectively exhibits scale invariance and it behaves in much the same way as if it were precisely at the quantum critical point. Both in this high frequency regime and at the quantum critical point the notion of a quasi-particle is, truly speaking, ill-defined, although for systems with small anomalous dimension  $\eta$  (the typical case for  $D \geq 2$ ) the continuum will often exhibit features (branch-points, not poles) whose dispersion resembles that of the Goldstone modes of the ordered phase.(49)

A classical critical point is described by thermodynamics alone, so none of these dynamical considerations affect the critical phenomena. In particular, it follows from the classical limit of the fluctuation-dissipation theorem that  $S(\mathbf{k}) = T\chi(\mathbf{k}, \omega = 0)$ , so  $S$  has the same critical behavior as the (static) susceptibility,  $\chi$ , even though  $S$  involves an integral over the dynamical structure factor at all frequencies. Consequently, a growing peak in  $S(\mathbf{k})$  at the ordering vector,  $\mathbf{k} = \mathbf{k}_{\text{ch}}$  with width  $|\mathbf{k} - \mathbf{k}_{\text{ch}}| \sim 1/\xi$ , and amplitude  $S(\mathbf{k}_{\text{ch}}) \sim |T - T_c|^{-\gamma}$  reflects the presence of fluctuating stripe order near a thermal transition. Here  $\gamma = \nu(2 - \eta)$  is typically about 1 or greater, so the amplitude is strongly enhanced.

The situation is quite different at a quantum critical point, where the dynamics and the thermodynamics are inextricably linked. Here, the fact that by far the largest contribution to  $S(\mathbf{k})$  comes from the high frequency multi-particle continuum which does not directly probe the fluctuating order means that the relevant structure in  $S(\mathbf{k})$  is relatively small, and can be very difficult to detect in practice. To see this, we compare the expressions in terms of the dissipative response function,  $\chi''(\mathbf{k}, \omega)$ , for the susceptibility (obtained from the Kramers-Krönig relation) and  $S(\mathbf{k})$  (obtained from the fluctuation-dissipation theorem):

$$\begin{aligned} \chi(\mathbf{k}, \omega = 0) &= \int \frac{d\omega}{2\pi} \chi''(\mathbf{k}, \omega)/\omega & (2.3) \\ S(\mathbf{k}) &= \int \frac{d\omega}{2\pi} \coth\left(\frac{\beta\hbar\omega}{2}\right) \chi''(\mathbf{k}, \omega) \end{aligned}$$

In the limit  $T \rightarrow 0$ ,  $\coth(\beta\hbar\omega) \rightarrow 1$ ; then clearly, the factor  $1/\omega$  weights the important low frequency part of the integral expression for  $\chi$  much more heavily than in the expression for  $S$ . Consequently, it follows under fairly general circumstances from the scaling form of  $\chi''$  that  $S(\mathbf{k}_{\text{ch}}) \sim \tau^{-1}\chi(\mathbf{k}_{\text{ch}})$ , or in other words that  $\chi(\mathbf{k}_{\text{ch}}) \sim \ell^{-\gamma}$  is strongly divergent in the neighborhood of the quantum critical point, while  $S(\mathbf{k}_{\text{ch}}) \sim \ell^{\nu z - \gamma} = \ell^{-\nu(2 - z - \eta)}$  is much more weakly divergent, or, if perchance  $z \geq 2 - \eta$ , not divergent at all.

At criticality ( $\ell = 0$ ) similar considerations imply that  $S(\mathbf{k}, \omega)$  is a less singular function at small momentum/frequency than the corresponding susceptibility (see Sec. III).

These considerations apply even on the ordered side of the quantum critical point, where the Bragg peak makes an exceedingly small (although sharp) contribution to the total structure factor which vanishes in proportion to  $\ell^{2\beta}$ . By contrast, the Bragg peak constitutes the entire contribution to  $S(\mathbf{k}, \omega = 0)$ , and is the dominant piece of the structure factor integrated over any small frequency window which includes  $\omega = 0$ .

**Lesson #1:** There is an important lesson concerning the best way to analyze experiments to be gleaned from this general discussion. It is the low frequency part of  $S(\mathbf{k}, \omega)$  which is most directly sensitive to the stripe order. Rather than analyze  $S(\mathbf{k})$ , information concerning local stripe order is best obtained by studying  $\chi(\mathbf{k}, \omega = 0)$  or by analyzing the partially-frequency-integrated spectral function,

$$\tilde{S}(\mathbf{k}, \Omega) \equiv (2\Omega)^{-1} \int_{-\Omega}^{\Omega} \frac{d\omega}{2\pi} S_{\text{ch}}(\mathbf{k}, \omega) \quad (2.4)$$

where on the ordered side of the critical point, the smaller  $\Omega$  the better, while on the quantum disordered side,  $\Omega$  must be taken larger than  $E_G/\hbar$ , but not more than a few times  $E_G/\hbar$ . This quantity is less severely contaminated by a “background” arising from the incoherent high energy excitations. As we will discuss in Sec. V.A, this is precisely the way local stripe order is best detected in clean, high temperature superconductors.

### C. How weak disorder can make life simpler

In the absence of quenched disorder, there is no useful information available from the structure factor at frequencies less than  $E_G$ , which means in particular that static experiments ( $\omega = 0$ ) are blind to fluctuating order. However, a small amount of quenched disorder, with characteristic energy scale  $V_{\text{dis}} \sim E_G$  but much smaller than the “bandwidth” of the continuum of the spectral function, has important effects on the low energy states. It is intuitively clear that induced low frequency structure of  $S(\mathbf{k}, \omega)$  will be largest for values of  $\mathbf{k}$  where, in the absence of disorder,  $S$  has spectral weight at the lowest frequencies, *i.e.* for  $\mathbf{k} \sim \mathbf{k}_{\text{ch}}$ . Although, the effects of quenched randomness on the pure critical theory can be subtle(50) and rarely well understood (unless disorder happens to be irrelevant) the generation of zero energy states is generic.

**Lesson # 2:** The upshot is that the effect of weak quenched disorder in a quantum disordered phase is to produce a low frequency “quasi-elastic” part of the spectral function  $S(\mathbf{k}, \omega)$ . In other words, disorder will eliminate the spectral gap, but will only weakly affect the partially integrated spectral function, Eq. (2.4), with the integration scale set by  $V_{\text{dis}}$ . In particular, in the presence of weak disorder, the static structure factor,  $S(\mathbf{k}, \omega = 0)$ , should exhibit similar  $\mathbf{k}$  dependence as  $\tilde{S}(\mathbf{k}, \Omega)$ , and so can be used to reveal the nature of the nearby ordered phase.

### D. Response functions

To formalize some of these notions, we consider the somewhat simpler problem of the response of the system to a weak, applied external field which couples to the order parameter. In a quantum disordered phase the existence of an order parameter can only be made apparent directly by coupling the system to a suitable symmetry-breaking field. For a charge-stripe smectic, a non-uniform potential couples to the order parameter and thus serves as a suitable symmetry breaking field. Thus, the Fourier component  $V_{\mathbf{k}}$  of a weak potential induces a non-vanishing expectation value of the order parameter which, in linear response, is

$$\langle \rho_{\mathbf{k}} \rangle = \chi_{\text{ch}}(\mathbf{k}) V_{\mathbf{k}} + \dots \quad (2.5)$$

The linear response law of Eq. (2.5) is valid provided  $V_{\mathbf{k}}$  is sufficiently small. However, if the typical magnitude of  $V$  with Fourier components in the range  $|\mathbf{k} - \mathbf{Q}_{\text{ch}}| \xi \lesssim 1$ ,  $\bar{V}_{\mathbf{k}_{\text{ch}}} \gtrsim E_G$ , the critical region is accessed and Eq. (2.5) is replaced by the law

$$\langle \rho_{\mathbf{k}_{\text{ch}}} \rangle \sim [\bar{V}_{\mathbf{k}_{\text{ch}}}]^{1/\delta} \quad (2.6)$$

where  $\delta = 2/(D - 2 + \eta)$  is another critical exponent.

Many local probes, including STM and NMR, are more sensitive to the (LDOS) local density of electronic states,  $\mathcal{N}(\mathbf{r}, E)$ . Again, in the quantum disordered state, translation invariance implies that, in the absence of an external perturbation,  $\mathcal{N}(\mathbf{r}, E) = \mathcal{N}_0(E)$  is independent of  $\mathbf{r}$ . In the presence of a weak potential, it is possible to define a relation for the local density of states

$$N(\mathbf{k}, E) = \chi_{\text{DOS}}(\mathbf{k}, E) V_{\mathbf{k}} + \dots \quad (2.7)$$

where  $N(\mathbf{k}, E)$  is the Fourier transform of  $\mathcal{N}(\mathbf{r}, E)$ . From linear response theory it follows that

$$\begin{aligned} \chi_{\text{DOS}}(\mathbf{k}, E) &= (2\pi)^{-1} \int d\mathbf{r} dt d\tau e^{iEt - i\mathbf{k} \cdot \mathbf{r}} \theta(\tau) \\ &\times \langle \{ \Psi_{\sigma}^{\dagger}(\mathbf{r}, t + \tau), \Psi_{\sigma}(\mathbf{r}, \tau) \}, \hat{n}(\mathbf{0}) \rangle \end{aligned} \quad (2.8)$$

where  $\theta$  is the Heaviside function,  $\Psi_{\sigma}^{\dagger}$  is the electron creation operator, and  $\hat{n} = \sum_{\sigma} \Psi_{\sigma}^{\dagger} \Psi_{\sigma}$  is the electron density operator. Note that, despite appearances,  $E$  is not a frequency variable, but is rather the energy at which the time independent density of states is measured. A simple sum-rule relates  $\chi_{\text{ch}}$  to  $\chi_{\text{DOS}}$ :

$$\chi_{\text{ch}}(\mathbf{k}) = \int dE f(E) \chi_{\text{DOS}}(\mathbf{k}, E) \quad (2.9)$$

where  $f(E)$  is the Fermi function.

It is also interesting to consider stripe orientational, or nematic, order. Since  $\chi_{\text{ch}}(\mathbf{k})$  is a property of the uniform fluid phase, it respects all the symmetries of the underlying crystal; in particular, if rotation by  $\pi/2$ , is a symmetry of the crystal, then  $\chi_{\text{ch}}(\mathbf{k}) = \chi_{\text{ch}}(\mathcal{R}[\mathbf{k}])$ , so no information about incipient nematic order can be obtained to linear order in the applied field. However, the

leading non-linear response yields a susceptibility for the nematic order parameter, defined in Eq. (2.1), as

$$\mathcal{Q}_{\mathbf{k}} = \int d\mathbf{p} \chi_{\text{nem}}(\mathbf{k}; \mathbf{p}) [V_{\mathbf{p}} - V_{\mathcal{R}[\mathbf{p}]}][V_{-\mathbf{p}} + V_{-\mathcal{R}[\mathbf{p}]}] + (2.10)$$

This non-linear susceptibility ( $\chi_{\text{nem}}$  contains a four-density correlator) diverges at the nematic to isotropic quantum critical point, and we would generally expect it to be largest for  $\mathbf{Q} \approx \mathbf{Q}_{\text{ch}}$ . It is important to note that the density modulations, reflecting the proximity of stripe order, are a first order effect, while the nematic response, which differentiates  $\mathbf{Q}_{\text{ch}}$  from  $\mathcal{R}[\mathbf{Q}_{\text{ch}}]$ , is second order, and so will tend to be weaker, even if the nematic quantum critical point is nearer at hand than that involving the stripe ordered state.

At a first level of approximation, it is possible to view weak quenched disorder as a random, applied field,  $V$ . Thus, the results of this subsection shed light on the weak disorder problem.

### E. Phase diagrams

When there is more than one competing ordered phase, the phase diagram can be very complicated, and moreover can be quite different, depending on various microscopic details. Nonetheless, it is often useful to have a concrete realization of the phase diagram in mind, especially when thinking about issues related to order, and order parameter fluctuations. In this subsection, we sketch schematic phase diagrams which characterize some of the ordered phases and fluctuation effects discussed above; the reader is cautioned, however, that the shape, topology, and even the number of ordered phases may vary for material-specific reasons.

Figure 1(a) represents the essential features we have in mind, in the absence of any quenched disorder. Here, there is a stripe ordered phase which occurs at low doping and low temperature, with a phase boundary which ends at a quantum critical point deep in the superconducting phase. In the region marked “fluctuating stripes,” there is significant local stripe order whose character is governed by the proximity to the quantum critical point. Notice that this fluctuation region extends into the stripe ordered phase itself; although there is true long-range stripe order in this region of the phase diagram, the degree of striping at the local level is much greater than the small ordered component close to the quantum critical point. There is no universal statement possible concerning how far the fluctuating stripe region extends beyond the ordered phase. Clearly, if the region in which there is *local* stripe order does not at least include the entire region of the phase diagram in which high temperature superconductivity occurs, it cannot be essential for the mechanism of superconductivity.

Under many circumstances, the stripe ordered phase will not end at a quantum critical point, but rather will terminate at a first order line(33). If the transition is

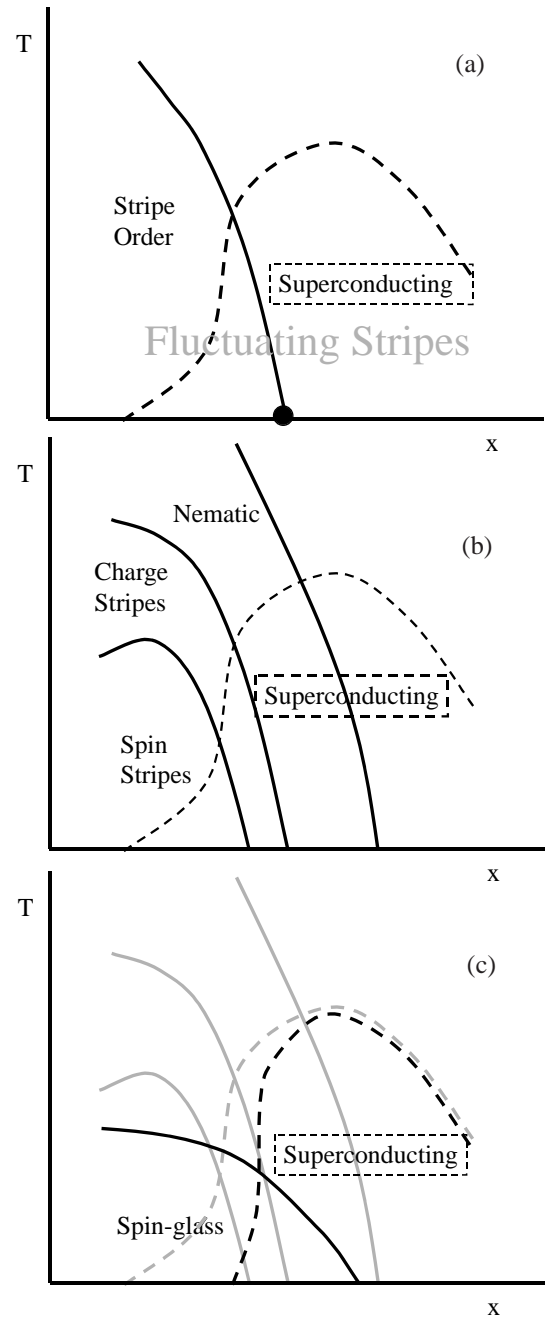


FIG. 1 Schematic phase diagrams showing various forms of stripe order, and its interactions with high temperature superconductivity; see text for discussion.

only weakly first order, this will not affect the general considerations presented here. If it is strongly first order, fluctuation effects are much weaker, and the effects of even very weak quenched disorder are much more severe than in the case of a continuous transition. We do not have much concrete to say about this latter case, although it is likely relevant to some systems, perhaps including the organic superconductors.(51)

Figure 1(b) is a more ornate version of the phase dia-

gram, in which all the different broken symmetry phases discussed in the present paper are exhibited. Here, we illustrate the case in which the nematic, charge, and spin ordering occur at distinct transitions, under which circumstances the nematic ordering must precede the charge ordering, which must in turn precede the spin ordering(42). In sketching the global shape of the phase diagram, we have included the prejudice that static stripe order, especially static spin-stripe order, competes strongly with superconductivity, but that a degree of local stripe order is necessary for high temperature pairing—the latter prejudice is reflected in the vanishing of the superconducting  $T_c$  as the local stripe order is suppressed upon overdoping. However, these prejudices affect only the interplay between stripe order and superconducting order in the phase diagram, and not the central features on which we focus in the present article, concerning the character of fluctuating stripe order. (In general, there are also distinctions between commensurate and incommensurate, diagonal and vertical, bond-centered and site centered stripe order, so the same general considerations could lead to significantly more complicated phase diagrams.)

The effect of an externally applied magnetic field on the competition between superconducting and stripe order has been treated recently in several papers.(54)

Finally, Fig. 1(c) shows the effect of weak disorder on the phase diagram illustrated in Fig. 1(b); all phase transitions involving breaking of spatial symmetries are rounded by quenched disorder, so the only true phase transitions are a superconducting and a spin-glass transition, although the spin-glass should have a local stripe character—it is(59) a “cluster spin glass.” Note that quenched disorder generally introduces some frustration(60), so where in the absence of quenched disorder the spin-freezing temperature is large, quenched disorder tends to suppress it. Conversely, where quantum fluctuations have destroyed the ordered state, the additional “pinning” effect of quenched disorder can lead to a spin-glass phase extending beyond the border that the magnetic phase would have in the zero disorder limit.

### III. ONE-DIMENSIONAL LUTTINGER LIQUID

In this section, we show how the general features described above play out in the case of the 1DEG. For simplicity, we present results for a spin-rotation-invariant Tomanaga-Luttinger liquid (TLL); in a forthcoming publication (61) we will provide details of the derivations, and will also discuss the Luther-Emery liquid (LEL), *i.e.* the spin-gap case. Both the TLL and the LEL are quantum critical (62) with  $z = 1$ . So long as the charge Luttinger parameter is in the range  $0 < K_c < 1$  (which is typically the case for repulsive interactions), the charge susceptibility of the TLL diverges as  $k \rightarrow 2k_F$  as

$$\chi(2k_F + q) \sim |q|^{K_c-1}. \quad (3.1)$$

This system can rightly be viewed as a quantum critical CDW state. (The CDW fluctuations are still stronger in the LEL case, where the susceptibility exponent is replaced by  $K_c - 2$ .) Thus, it is the perfect laboratory for testing the validity of the general scaling considerations of Section II.

The charge density structure factor of the TLL is the Fourier transform of the more readily evaluated space time structure factor

$$S(k, \omega) = \int_{-\infty}^{\infty} dt \int_{-\infty}^{\infty} dx \mathcal{S}(x, t) e^{ikx - i\omega t} \quad (3.2)$$

where the charge correlation function  $\tilde{S}(r, t)$  is given by

$$\begin{aligned} \mathcal{S}(r, t) = & \mathcal{S}_0(r, t) + [e^{i2k_F r} \mathcal{S}_{2k_F}(r, t) + \text{c.c.}] \\ & + [e^{i4k_F r} \mathcal{S}_{4k_F}(r, t) + \text{c.c.}] + \dots \end{aligned} \quad (3.3)$$

where explicit expressions for  $\mathcal{S}_0$ ,  $\mathcal{S}_{2k_F}$ , etc. are given in the literature.(62) These expressions can be Fourier transformed (although in general, this must be done numerically) to yield expressions for the dynamical structure factor. Since the LL is quantum critical, this (and other) correlation functions have a scaling form; for example, near  $2k_F$  (*i.e.* for small  $q$ )

$$S(2k_F + q, \omega) = \frac{1}{v_c} \left( \frac{D}{\hbar v_c q} \right)^a \Phi_{2k_F} \left( \frac{\omega}{v_c q}, \frac{\hbar \omega}{k_B T} \right) \quad (3.4)$$

where  $a = 1 - K_c$  and  $D$  is an ultraviolet cutoff, *i.e.* the bandwidth of the TLL.  $\Phi_{2k_F}$  depends implicitly on the dimensionless parameters  $K_c$  and  $\frac{v_c}{v_s}$  with  $v_c$  and  $v_s$  respectively, the charge and spin velocities,. (Spin rotation invariance constrains the spin Luttinger exponent  $K_s$  to be equal to 1.) To exhibit the general features we are interested in, while making the Fourier transform as simple as possible, we can consider the limit  $T = 0$  and set  $v_s = v_c = v$ . Then, for  $q$  small,

$$S(2k_F + q, \omega) \sim \frac{1}{v} \left( \frac{D}{\hbar v q} \right)^a \theta \left( \frac{\omega^2}{v^2 q^2} - 1 \right) \left[ \frac{\omega^2}{v^2 q^2} - 1 \right]^{\frac{K_c-1}{2}} \quad (3.5)$$

where  $\theta(x)$  is the step function.

For fixed  $\omega$ , as a function of  $q$ , the dynamic structure factor exhibits a multi-particle continuum for  $-\omega/v \leq q \leq \omega/v$ , but it does have singular structure, which can be thought as an image of the Goldstone (phason) modes one would find were there true CDW order:

$$S(2k_F + q, \omega) \sim [\omega - v|q|]^{(K_c-1)/2} \quad \text{as } |q| \rightarrow \omega/v \quad (3.6)$$

The equal time structure factor can also be readily computed by integrating the dynamical structure factor; as  $q \rightarrow 0$

$$S(2k_F + q) \sim A - A' (q\alpha/2)^{K_c} \quad (3.7)$$

where  $A$  and  $A'$  are numbers of order 1 and  $\alpha$  is a short distance cutoff which we take to be  $\alpha \sim v/D$ .

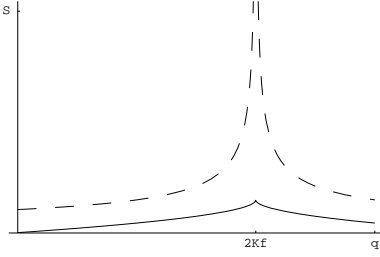


FIG. 2 The  $T = 0$  charge structure factor,  $S(k)$  (solid line), and the static susceptibility,  $\chi(k, \omega = 0)$  (dashed line), of the TLL with  $v_s = v_c$  and  $K_c = 0.5$ .

As promised, this singularity is much weaker than that exhibited by  $\chi$ , and indeed the  $2k_F$  component of the structure factor remains finite (but not differentiable) as  $q \rightarrow 0$ . ( See Fig. 2.)

We now turn to the spatial structure induced by a single impurity in the 1DEG, which we locate at the origin. For a Luttinger liquid with repulsive interactions the charge Luttinger parameter  $K_c$  lies in the range  $0 < K_c < 1$ . For  $K_c$  in this range, the  $2k_F$  component of an impurity potential, whose amplitude we will denote by  $\Gamma$ , is a relevant perturbation (65) with (boundary) scaling dimension  $d = \frac{1}{2}(K_c + 1)$ . Thus, there is a crossover energy scale  $T_K \propto \Gamma^{2/(1-K_c)}$  such that excitations with energy large compared to  $T_K$  see a weak backscattering potential, and are thus only weakly perturbed by the impurity. Conversely, for energies low compared to  $T_K$  the system is controlled (65) by the fixed point at  $\Gamma \rightarrow \infty$ . However, at this fixed point, the high energy cutoff is replaced by a renormalized cutoff,  $D \rightarrow T_K$ .

We begin, therefore, by considering the limit  $\Gamma = \infty$ , *i.e.* a semi-infinite system with  $x \geq 0$  and the boundary condition that no current can flow past  $x = 0$ . This solution is accurate for all energies  $|E| \ll T_K$ . The Fourier transform of the impurity induced DOS

$$N(k, E) = \frac{1}{2\pi} \int_{-\infty}^{\infty} dt \int_0^{\infty} dx [g^>(x, t) + g^<(x, t)] e^{i(Et - kx)} \quad (3.8)$$

can be computed using exact expressions for the appropriate single particle Green function (66):

$$\begin{aligned} g^>(x, x; t) &= \sum_{\sigma} \langle \Psi_{\sigma}^{\dagger}(x, t) \Psi_{\sigma}(x, 0) \rangle \equiv g(x, t) \quad (3.9) \\ &= g_0(x, t) + [e^{i2k_F x} \tilde{g}_{2k_F}(x, t) + e^{-i2k_F x} \tilde{g}_{2k_F}(-x, t)] + \dots \end{aligned}$$

where  $g_0(x, t)$  is the long wavelength part and  $g_{2k_F}(x, t)$  is the  $2k_F$  part. We will be interested in the  $2k_F$  component which clearly contains information about CDW correlations in this semi-infinite 1DEG, and for which a general expression in space and time has been given by Eggert and others (66).  $2k_F$  part of  $N(k, E)$  can be ex-

pressed in terms of the scaling function  $\Phi$  as

$$N(q + 2k_F, E) = \frac{\hbar B}{E} \left( \frac{E}{D} \right)^{2b} \Phi \left( \frac{2E}{\hbar v_c q}, \frac{E}{k_B T} \right) \quad (3.10)$$

where  $b = (1 - K_c)^2 / 4K_c$  and  $B$  is a dimensionless constant; we have left implicit the dependence on the dimensionless parameters  $K_c$  and  $v_c/v_s$ .

The scaling form of  $N(k, E)$ , given in Eq. 3.10, expresses that fact that the Luttinger liquid is a quantum critical system. The spectrum of the Luttinger liquid and the existence of a charge-ordered state induced by the impurity, dictate entirely the structure of the scaling function  $\Phi(x, y)$ : it has a multi-soliton continuum for both right and left moving excitations, each with leading thresholds associated with one-soliton states carrying separate spin and charge quantum numbers and moving at their respective velocities, as well as a non-propagating feature associated with the pinning of the CDW order by the impurity. Thus, the STM spectrum exhibits all the striking features of the Luttinger liquid: spin-charge separation and quantum criticality, *i.e.* fluctuating order. The beauty of the 1DEG is that much of this can be worked out explicitly.

In Figs. 3a and 3c, we show the scaling function computed numerically for various representative values of the parameters. The plots show the real and imaginary parts of  $N(2k_F + q, E)$  at fixed  $E/k_B T$  as a function of the scaled momentum,  $\hbar v_c q / k_B T$ , for  $|q| \ll k_F$ . For comparison, we also show (129) in Figs. 3b and 3d, the single particle spectral function  $A(k_F + q, \omega)$  that would be measured in an angle resolved photoemission experiment (ARPES) on the same system in the absence of an impurity. There are several things to note about these plots: **1)** Because of the quantum critical scaling form, high energy and low temperature are equivalent. Note, however, that in interpreting the large  $E/k_B T$  spectra as representative of the low temperature behavior of the system, it is important to remember that the thermal scaling of the  $k$ -axis of the figure hides the fact that all features of the spectrum are becoming sharper as  $T \rightarrow 0$ ; this is made apparent in Fig. 4. **2)** It is clear that there are right dispersing features of the scaling functions characterized by the spin and charge velocities. The interference between dispersing features of the ARPES spectrum near  $k_F$  and  $-k_F$  can be loosely thought of as giving rise to the dispersing features in the STM spectrum; indeed, as  $K_c \rightarrow 1$  (the non-interacting limit), it is easy to show that  $\text{Re}\{N(2k_F + q, E)\} \propto A(k_F + q/2, E)$ . However, it is also clear from the figure that the stronger the interactions, the less direct is the resemblance between  $N(2k_F + q, E)$  and  $A(k_F + q/2, E)$ . **3)** There is also a very weak feature in the spectrum, visible only at quite large  $E/k_B T$  (compare Figs. 3 and 4), which disperses in the opposite direction (left) to the main features of the spectra with velocity  $-v_c$ . Because these spectra are shown only for  $k$ 's in the neighborhood of  $+2k_F$  (or  $+k_F$  for  $A(k, E)$ ), there is no symmetry between right and left moving excitations. If we showed the spectra on a larger scale, there

would of course be the mirror symmetric spectra near  $-2k_F$  (or  $-k_F$ ) as required by Kramer's theorem. **4)** In the STM spectrum, but not in the ARPES spectrum, there is a feature near  $q = 0$  which does not disperse strongly with increasing energy; this is directly related to the pinned CDW order. Note that for  $K_c = 0.5$ , this feature is weak in Fig. 3, and only becomes prominent at very large  $E/k_B T$ , as shown in Fig. 4; but this is the most important feature of the data if one is interested in evidence of pinned CDW order.

To further illustrate these points, we have obtained analytic expressions for the singular pieces of  $N(k, E)$  at  $T = 0$ , for a general value of the charge Luttinger parameter in the range of interest  $0 < K_c < 1$ , and general  $v_c/v_s$ .  $N(k, E)$  has power law singularities as  $2E/\hbar v_c q \rightarrow \pm 1$ ,  $2E/\hbar v_c q \rightarrow 0$ , and  $2E/\hbar v_c q \rightarrow \infty$  and  $2E/\hbar v_c q \rightarrow v_s/v_c$ . Physically the non-analyticities at  $2E/\hbar v_c q = \pm 1$  and  $2E/\hbar v_s q = 1$  represent the threshold of the continuum of propagating excitations moving to the right and to the left respectively. The singularity at  $2E/\hbar v_c q \rightarrow \infty$  corresponds to the  $2k_F$  CDW stabilized (pinned) by the boundary. Close to the right dispersing charge-related singularity at  $q \rightarrow 2E/\hbar v_c$  we find

$$N(2k_F + q, E) \sim \frac{\hbar}{2E} \left( \frac{2E}{D} \right)^{2b} A_+ \left[ 1 - \frac{2E}{\hbar v_c q} \right]^{b-1/2} \quad (3.11)$$

where  $A_+$  is a finite complex coefficient determined by the strength of the singularity. An important feature of this result is that as  $E$  goes through this singularity at fixed  $q$ , the phase of  $N(2k_F + q, E)$  jumps by  $\pi(b - 1/2)$ . (See Fig. 4.) Close to the right dispersing spin-related singularity at  $q \rightarrow 2E/\hbar v_s$  we find

$$N(2k_F + q, E) \sim \frac{\hbar}{2E} \left( \frac{2E}{D} \right)^{2b} A'_+ \left[ 1 - \frac{2E}{\hbar v_s q} \right]^{2b-1/2} \quad (3.12)$$

where  $A'_+$  is another complex coefficient. In the non-interacting limit  $K_c = 1$  and  $v_s = v_c$ , these two singularities coalesce into a simple pole for a particle moving to the right. However, for  $K_c < 1$ , the TLL does not have quasi-particles but massless soliton states instead. As usual, the power laws reflect the multi-soliton continuum. (More generally, the limit  $v_s/v_c \rightarrow 1$  is somewhat subtle(61).) Similarly, for  $q \rightarrow -2E/\hbar v_c$

$$N(2k_F + q, E) \sim \frac{\hbar}{2E} \left( \frac{2E}{D} \right)^{2b} A_- \left[ 1 + \frac{2E}{\hbar v_c q} \right]^b \quad (3.13)$$

where, once again,  $A_-$  is a finite complex coefficient specific to this singularity. However, unlike the singularity at  $E = +\hbar v_c q$ , the behavior near  $E = -\hbar v_c q$  although non-analytic is not divergent since  $b > 0$  for repulsive interactions.

**Lesson #3:** From this explicit example we learn that dispersing features in an STM measurement that resemble the interference effects that arise from non-interacting quasiparticles do not necessarily imply the existence of well defined quasiparticles!

In addition to propagating excitations, we also find that  $N(2k_F + q, E)$  has a singularity associated with the non-propagating CDW as  $q \rightarrow 0$ ;

$$N(2k_F + q, E) \sim \frac{\hbar}{2E} \left( \frac{2E}{D} \right)^{2b} A \left[ \frac{2E}{\hbar v_c q} \right]^{(1-K_c)/2} \quad (3.14)$$

which diverges as  $q \rightarrow 0$ . This singularity also exhibits a phase jump as  $q \rightarrow 0^\pm$ , equal to  $\pi(1 - K_c)/2$ .

Finally, at low voltages  $E \rightarrow 0$  and at fixed  $q$ , we find

$$N(2k_F + q, E) \sim \frac{\hbar}{2E} \left( \frac{2E}{D} \right)^{2b} \left[ \frac{2E}{\hbar v_c q} \right]^{c+1}. \quad (3.15)$$

where  $c = (1 - K_c^2)/4K_c$ .

It is interesting to compare  $N(k, E)$  with the DOS averaged over some energy scale,

$$\tilde{N}(2k_F + q, E) \equiv E^{-1} \int_{-E}^0 d\epsilon N(2k_F + q, \epsilon). \quad (3.16)$$

Note that at  $T = 0$ ,  $E\tilde{N}(k, E) \rightarrow \langle \rho_k \rangle$  as  $E \rightarrow \infty$ . However, the expression we have used for  $N(k, E)$  was derived for an infinite strength scattering potential, and so is only valid up to energies of the order of  $T_K \ll D$ . This condition is met by taking  $1/T_K$  as a short-time cutoff needed to compute the “almost equal-time” Green's function. This integrated quantity is shown in Fig. 5 for representative parameters. at  $T = 0$ , and in the limit as  $q \rightarrow 0$ ,  $\tilde{N}(2k_F + q, T_K)$  has the asymptotic behavior

$$\tilde{N}(2k_F + q, T_K) \sim \left( \frac{T_K}{v_c} \right) \left( \frac{T_K}{D} \right)^{-2b} \left( \frac{T_K}{v_c q} \right)^{-(1-K_c)/2}. \quad (3.17)$$

Both the integrated induced tunneling density of states and the induced tunneling density of states at fixed voltage  $E$  diverge like  $q^{-(1-K_c)/2}$ . However, the big difference is that  $N(k, E)$  has dispersing singularities in addition to the non-dispersing singularity at  $k \rightarrow 2k_F$ , while singularity at  $k \rightarrow 2k_F$  is the only singular feature of  $\tilde{N}(k, E)$ . Thus,  $\tilde{N}(k, T_K)$  is more easily analyzed for evidence of an almost ordered CDW state.

At energies  $E > T_K$ , the response of the system to the presence of the impurity is weak (*i.e.* proportional to  $\Gamma$ ), and can be computed in perturbation theory. For instance, in the weak impurity limit  $T_K \rightarrow 0$  the integrated response of the system over all energies is dominated by the high energy, perturbative regime where at  $T = 0$  we find

$$\tilde{N}(2k_F + q, D) \sim \left( 1 - \frac{2}{\mu} \left( \frac{\hbar v q}{2D} \right)^\mu + \dots \right) \Gamma + O(\Gamma^2) \quad (3.18)$$

where  $\mu = 1 + \frac{1}{4} \left( K_c - \frac{1}{K_c} \right)$ . This behavior applies for the regime  $q \gg k_B T_K/\hbar v$ .

It is also worth noting that the impurity induced local DOS at a fixed finite distance  $x$  from the impurity

$$\delta\mathcal{N}(x, E) \sim E^{(1-K_c)/2K_c}. \quad (3.19)$$

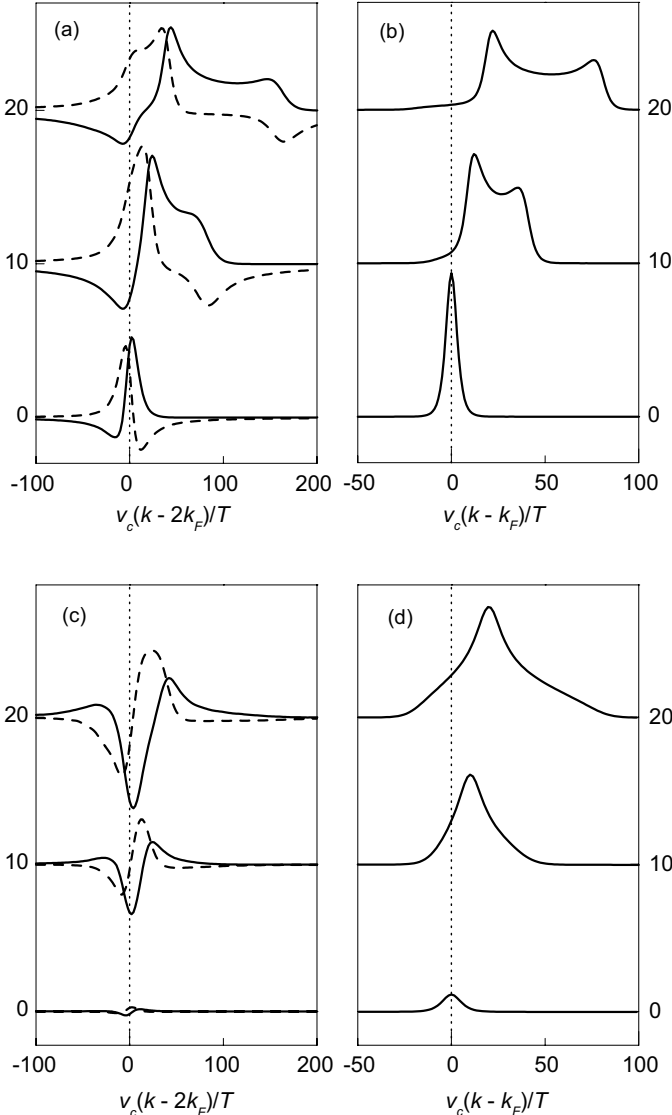


FIG. 3 Thermally scaled STM spectra  $N(k, E)$  in the neighborhood of  $k = 2k_F$  - (a) and (c) - and ARPES spectra - (b) and (d) - near  $k = k_F$ . In all cases,  $v_c/v_s = 4$  and  $K_s = 1$ ; for (a) and (b),  $K_c = 0.5$  ( $b = 1/16$ ) while for (c) and (d)  $K_c = 0.17$  ( $b = 1/2$ ). In (a) and (c), the density of states oscillations are induced by an impurity scatterer at the origin with  $T_K \gg E$ . In the STM spectra, the real and imaginary parts are represented by the solid and dashed lines, respectively. The curves are offset by  $E/T$  and we have adopted units  $\hbar = 1$  and  $k_B = 1$ .

is always large at low energies  $|E| \ll v/x$  compared to the background DOS of the clean TLL

$$\mathcal{N}(E) \sim E^{\frac{(1-K_c)^2}{4K_c}}. \quad (3.20)$$

This is yet another illustration of the way impurities enhance the low energy effects of fluctuating order.

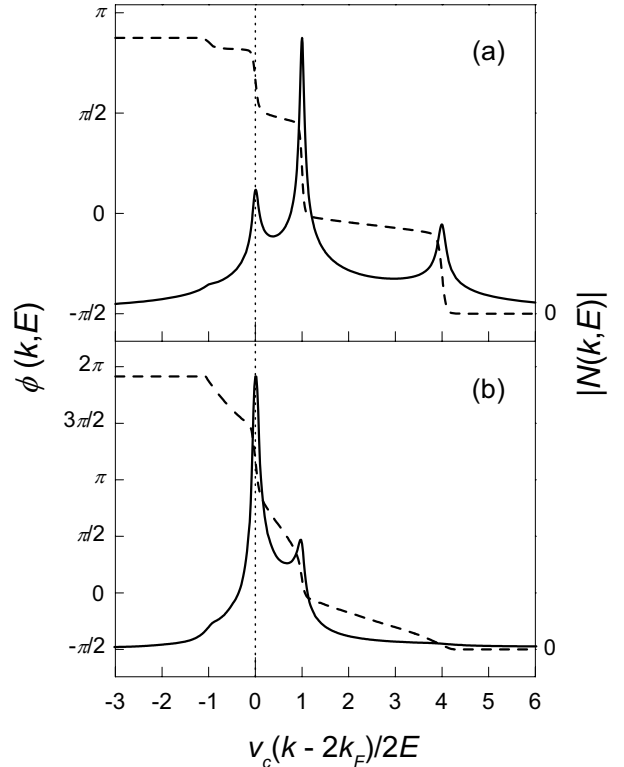


FIG. 4 Low temperature ( $E/k_B T = 100$ ) form of the STM spectra with  $k$  near  $2k_F$  for the same parameters as in Fig. 3; a) is for  $K_c = 0.5$  and b)  $K_c = 0.17$ . Here, we have expressed  $N(k, E) = |N(k, E)| \exp[i\phi(k, E)]$  where the amplitude is shown as a solid line and the phase as a dashed line.

#### IV. TWO-DIMENSIONAL FERMI LIQUID

As a final example, we consider the application of these ideas to the case of weakly interacting electrons in 2D. To obtain explicit results, we will consider electrons with a quadratic dispersion  $\epsilon_{\mathbf{k}} = \hbar^2 \mathbf{k}^2/2m$ .

Consider for instance  $\chi_{\text{DOS}}(E, \mathbf{k})$ , the new susceptibility defined in Eq. (2.8). We find that for the 2DEG it is given by

$$\chi_0(\mathbf{k}, E) = \frac{m}{\pi \hbar^2} \frac{\theta(\epsilon_{\mathbf{k}} - 4E)}{\sqrt{\epsilon_{\mathbf{k}}(\epsilon_{\mathbf{k}} - 4E)}} \quad (4.1)$$

Here, the subscript 0 is introduced for later convenience to signify  $\chi$  in the non-interacting limit, and once again  $\theta(x)$  is the Heaviside (step) function. For fixed  $E$  as a function of  $\mathbf{k}$ , this quantity diverges along curves in  $\mathbf{k}$  space where  $\epsilon_{\mathbf{k}} = 4E$  ( $|\mathbf{k}| = 2k_F$ ). Note that the fact that  $\chi_0$  vanishes for  $\epsilon_{\mathbf{k}} < 4E$  is a peculiarity of the 2D case with infinite quasiparticle lifetime. For instance, in 3D,

$$\chi_0(\mathbf{k}, E) = \frac{1}{8\pi^2} \left( \frac{2m}{\hbar^2} \right)^{3/2} \frac{1}{\sqrt{\epsilon_{\mathbf{k}}}} \ln \left| \frac{2\sqrt{E} + \sqrt{\epsilon_{\mathbf{k}}}}{2\sqrt{E} - \sqrt{\epsilon_{\mathbf{k}}}} \right| \quad (4.2)$$

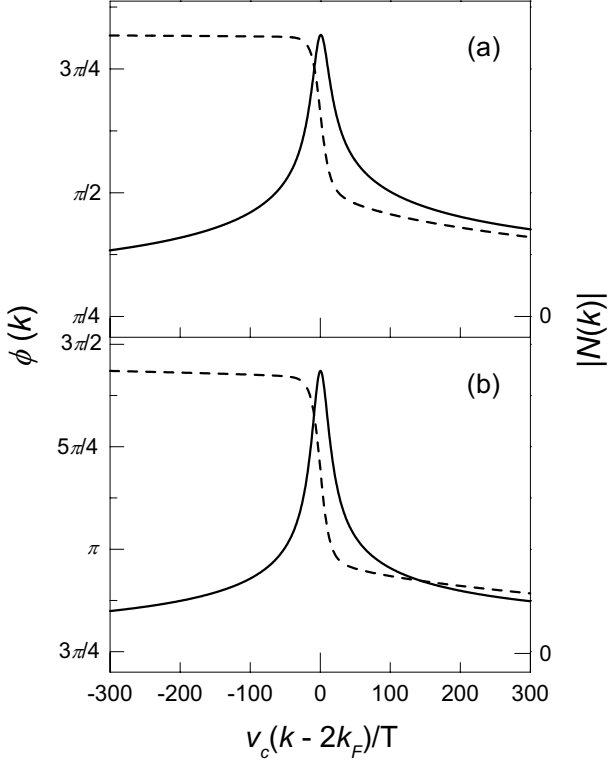


FIG. 5 Thermally scaled integrated STM spectra  $\tilde{N}(k, T_K)$  in the neighborhood of  $k = 2k_F$  for  $v_c/v_s = 4$  and  $K_s = 1$  with a)  $K_c = 0.5$  and b)  $K_c = 0.17$ . The solid line is the amplitude and the dashed line is the phase. (For a caveat, see Ref. (130).)

which also has a singularity as  $\epsilon_{\mathbf{k}} \rightarrow 4E$ , but is non-zero (and positive) for all  $E > 0$ . In contrast, as shown in Section III, in a 1D Luttinger liquid the induced density of states has a phase jump as  $k$  crosses any of the propagating or non-propagating singularities. It is straightforward to see that both in 2D and the 3D a finite lifetime of the quasiparticles leads to a rounding of the singularities and that in 2D it also leads to a positive induced density of states for all  $E > 0$ . It is also simple to verify that to non-linear order in the external potential, the induced density of states in 2D may or may not have a phase jump across the singularity depending on the details of the perturbing potential. For instance, the induced DOS produced by a single impurity can be computed (from the impurity t-matrix); it exhibits sign reversal ( $\pi$  phase shift) across the singularity at  $\epsilon_{\mathbf{k}} = 4E$  for a repulsive potential, but not for an attractive one. In contrast, any  $b/f/k$  space structure that arises from proximity to a quantum critical point is derived from the susceptibility,  $\chi(\mathbf{k})$ , which is real and positive, so it always produces a signal whose phase is constant. (See below.)

**Lesson # 4:** The density of states modulations induced by weak disorder in a non-interacting metal are quite dif-

ferent in character from those expected from the proximity to a CDW quantum critical point, both in that they disperse strongly as a function of energy, and the peak intensities lie along curves (surfaces in 3D) in  $\mathbf{k}$  space, as opposed to the structure associated with isolated points in  $\mathbf{k}$  space expected from near critical fluctuations(67).

The charge susceptibility itself,  $\chi_0(\mathbf{k})$ , is well known from many studies of the 2DEG. It has an extremely weak non-analyticity, whenever  $|\mathbf{q}| = 2k_F$

$$\chi_0(\mathbf{q}) = \frac{m}{2\pi\hbar^2} \left( 1 - \theta(q - 2k_F) \sqrt{1 - \frac{4k_F^2}{q^2}} \right) \quad (4.3)$$

The inverse Fourier transform of this meager non-analyticity is what gives rise to the famous Friedel oscillations in the neighborhood of an isolated impurity,

$$\langle \rho(r) \rangle \sim \cos(2k_F r + \phi)/r^2. \quad (4.4)$$

What this means is that, for all intensive purposes, the Friedel oscillations are all but invisible in the Fourier transform of any conceivable STM experiment on a simple metal in  $D > 1$ . Some non-trivial method of data analysis is necessary, instead.(69)

It is worthwhile considering the effects of interactions on this picture. For weak enough interactions, the effects can be treated in a Hartree-Fock approximation. Thus, if we absorb any interaction induced changes in the band parameters into a renormalized band structure, the only change in the above analysis is that the external perturbation,  $V_{\mathbf{k}}$  in Eqs. 2.5 and 2.7 must be replaced by an effective potential,  $V_{\mathbf{k}} \rightarrow V_{\mathbf{k}} + U_{\mathbf{k}}\rho_{\mathbf{k}}$ , where  $U$  (which can be weakly  $\mathbf{k}$  dependent) is the strength of the electron-electron repulsion. This leads to the usual RPA expression for the susceptibilities of the interacting system, and to

$$\begin{aligned} \chi_{\text{ch}}(\mathbf{k}) &= [1 - U_{\mathbf{k}}\chi_0(\mathbf{k})]^{-1}\chi_0(\mathbf{k}) \\ \chi_{\text{DOS}}(\mathbf{k}, E) &= [1 - U_{\mathbf{k}}\chi_0(\mathbf{k})]^{-1}\chi_0(\mathbf{k}, E). \end{aligned} \quad (4.5)$$

(It is the fact that  $E$  is a probe energy, not a frequency, which is responsible for the fact that it is simply  $\chi_0(\mathbf{k})$ , rather than a frequency dependent factor, which appears in the expression for  $\chi_{\text{DOS}}(\mathbf{k}, E)$ .) Not surprisingly, since  $\chi_0(\mathbf{k})$  is finite for all  $\mathbf{k}$ , for small  $U$  there is little qualitative difference between  $\chi_0(\mathbf{k})$  and  $\chi(\mathbf{k})$ . However, if we imagine, as is often done (although we are not aware of any reason it is justified) that this RPA expression applies qualitatively for larger magnitude of  $U$ , then as a function of increasing magnitude of  $U$  we would eventually satisfy a Stoner criterion for CDW  $U_{\mathbf{k}}\chi(\mathbf{k}) = 1$ . Here, due to the relatively weak  $\mathbf{k}$  dependence of  $\chi_0$ , the CDW ordering vector  $\mathbf{Q}_{\text{ch}}$  is determined as much by the  $\mathbf{k}$  dependence of  $U$  as by effects intrinsic to the 2DEG.

Following this line of analysis, let us consider the behavior of  $\chi_{\text{DOS}}(\mathbf{k}, E)$  in the quantum disordered phase close to such a putative Stoner instability. Then, for  $\mathbf{k}$  close to  $\mathbf{Q}$ , the  $\mathbf{k}$  dependence comes primarily from the

first term, while the voltage dependence comes primarily from the band-structure:

$$\chi_{DOS}(\mathbf{k}, E) \approx [1 - U_{\mathbf{k}}\chi_0(\mathbf{k})]^{-1}\chi_0(\mathbf{Q}_{ch}, E). \quad (4.6)$$

Conversely, for  $\mathbf{k}$  far from the ordering vector, both the  $\mathbf{k}$  and  $E$  dependence of  $\chi$  are determined largely by  $\chi_0$ .

Although the calculations are somewhat more involved (and therefore must be implemented numerically), the same sort of weak coupling analysis can be carried out in the superconducting state. Oscillations induced by a mean-field with period 4, representing stripes with various internal structures in a d-wave superconductor, were carried out by Podolsky *et al.*(70). As expected, the stripes induce oscillations in the LDOS with the period 4, but with energy dependences which reflect both the quasi-particle dispersion, and the specific stripe structure assumed. Impurity induced oscillations in the LDOS in a d-wave superconductor were computed by Byers *et al.*(71) and Wang and Lee(68), and the effects of proximity to a stripe ordered state, at RPA level, were investigated by Polkovnikov *et al.*(72). In all cases, the interference and the stripe related effects interact in fairly complex ways, that require detailed analysis to disentangle.

**Lesson #5:** Thus, depending on what regions of  $\mathbf{k}$  space are probed, the STM spectrum can either be dominated largely by band-structure effects, or by the incipient CDW order. The most singular enhancement of the STM signal is expected to occur at energies such that a dispersing feature reflecting the underlying band-structure passes through the ordering wave-vector.

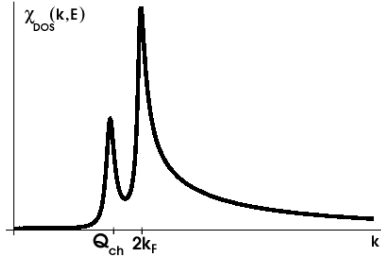


FIG. 6 The RPA expression for  $\chi_{DOS}(\mathbf{k}, E)$  is plotted as a function of momentum at a fixed, low energy  $E - \mu = .2\mu$ . A small decay rate,  $\Gamma = .025\mu$ , is included to round the singularity and produce a finite  $\chi_0(k, E)$  at all  $k$ . We have taken the following phenomenological form for  $\chi(\mathbf{k}) = A(\xi k_F)^2 \exp[-\xi 2(k - Q_{ch})^2]$  written in terms of  $\xi$  - the correlation length of CDW order (appropriate for  $\gamma = 2$ ). The figure was plotted with  $\xi = 5k_F^{-1}$  and  $Q_{ch} = 1.8k_F$ .

## V. REGARDING EXPERIMENTS IN THE CUPRATES

Even where broken symmetry associated with stripe order has ultimately been proven to exist, establishing

this fact has often turned out to be difficult for a number of practical reasons. In addition, since quenched disorder is always a relevant perturbation (in renormalization group sense), macroscopic manifestations of broken spatial symmetries are sharply defined only in the zero disorder limit. Nevertheless, the existence of some form of order which coexists with superconductivity has implications for the phase diagram which can, in principle and sometimes in practice, be tested by macroscopic measurements. A particularly revealing set of phenomena occur when the strength of the superconducting order is modulated by the application of an external magnetic field.(31; 38; 55; 56; 57; 58; 72; 73; 74; 75; 76; 77; 78) Moreover, as discussed in Sec. V.C, from measurements of macroscopic transport anisotropies, electronic nematic order (e.g., point-group symmetry breaking) has been identified beyond all reasonable doubt in quantum Hall systems,(79) and very compelling evidence for its existence has been reported in the last year in underdoped  $\text{La}_{2-x}\text{Sr}_x\text{CuO}_4$  and  $\text{YBa}_2\text{Cu}_3\text{O}_{6+y}$ .(78; 80)

However, most searches for stripe order rely on more microscopic measurements, especially elastic neutron scattering. One aspect of this that has caused considerable confusion is that, unless an external perturbation (such as weak crystalline orthorhombicity) aligns the stripes in one direction, one generally finds equal numbers of  $y$  directed and  $x$  directed domains, leading to quartets of apparently equivalent Bragg peaks, rather than the expected pairs. Fortunately, where sufficiently long-ranged order exists, it is possible, by carefully analyzing the scattering data, to distinguish this situation from a situation in which the peaks arise from a more symmetric “checker-board” pattern of translation symmetry breaking. From elastic neutron scattering (*i.e.*, measurements of both the magnetic and the nuclear  $S(\mathbf{k}, \omega = 0)$ ), and to a lesser extent from X-ray scattering, it has been possible to establish the existence of stripe-ordered phases in a wide range of members of the lanthanum cuprate family of high temperature superconductors:  $\text{La}_{1.6-x}\text{Nd}_{0.4}\text{Sr}_x\text{CuO}_4$  over the whole range of doped hole concentrations from  $0.05 < x \leq 0.2$  (Ref. 81; 82; 83),  $\text{La}_{2-x}\text{Ba}_x\text{CuO}_4$  (Ref. 84),  $\text{La}_{2-x}\text{Sr}_x\text{CuO}_4$  for  $0.02 < x < 0.13$  (Ref. 83; 85; 86; 87; 88; 89), and  $\text{La}_2\text{CuO}_{4+\delta}$  (Ref. 90, including optimally doped material with a doped hole concentration  $\approx 0.15$  and a superconducting  $T_c$  of 42 K). Exciting preliminary evidence of charge stripe order has been recently reported, as well, from elastic neutron scattering studies on underdoped  $\text{YBa}_2\text{Cu}_3\text{O}_{6+y}$  (with  $y = 0.35$  and  $T_c = 39$  K, Ref. 91) and optimally doped  $\text{YBa}_2\text{Cu}_3\text{O}_{6+y}$  (with  $y = 0.93$  and  $T_c = 93$  K, Ref. 92). And, it is worth mentioning, stripe order has also been similarly detected in a number of non-superconducting doped antiferromagnets, including  $\text{La}_{2-x}\text{Sr}_x\text{NiO}_{4+\delta}$  (Ref. 93; 94; 95; 96) and the colossal magneto-resistance manganites.(97; 98; 99; 100)

We now turn to the core problem: Given a system which in the absence of quenched disorder or explicit symmetry breaking terms is in an isotropic fluid state,

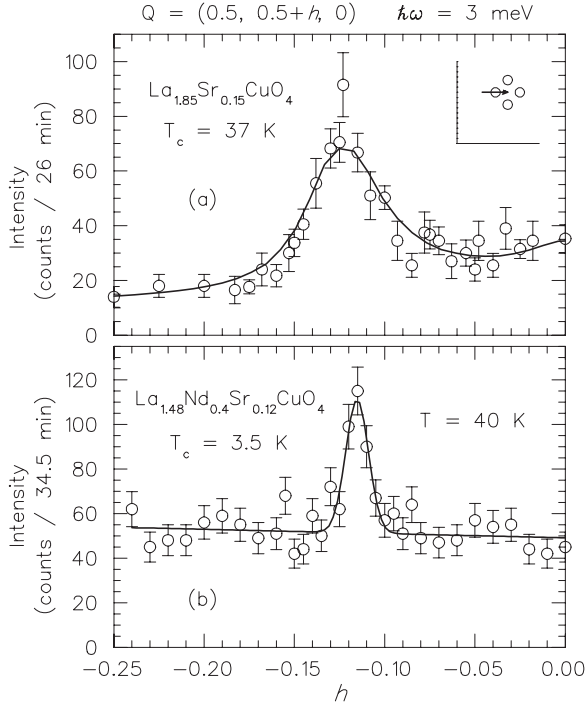


FIG. 7 Comparison of constant-energy scans at  $\hbar\omega = 3$  meV through an incommensurate magnetic peak (along path shown in inset) for (a)  $\text{La}_{1.85}\text{Sr}_{0.15}\text{CuO}_4$  and (b)  $\text{La}_{1.48}\text{Nd}_{0.4}\text{Sr}_{0.12}\text{CuO}_4$ . Both scans are at  $T = 40$  K  $> T_c$ . Measurement conditions are described in Ref. 101.

how is the existence of substantial local stripe order identified?

### A. Diffraction from stripes

Peaks in  $S(\mathbf{k}, \omega)$  at the characteristic stripe ordering vectors indicate a degree of local stripe order. The  $k$  width of these peaks can be interpreted as an indication of the spatial extent of local stripe order, and the low frequency cutoff as an indication of the typical stripe fluctuation frequency. So long as there is no spontaneous symmetry breaking,  $S(\mathbf{k}, \omega)$  necessarily respects all the point-group symmetries of the crystal, and thus will necessarily always show peaks at quartets of  $\mathbf{k}$  values, never the pairs of  $\mathbf{k}$  values of a single-domain stripe ordered state.

Low frequency spin fluctuations with relatively sharp peaks at incommensurate wave vectors were detected many years ago in inelastic neutron scattering studies(102; 103; 104) of “optimally-doped” ( $x \approx 0.15$ ,  $T_c \sim 38$  K)  $\text{La}_{2-x}\text{Sr}_x\text{CuO}_4$ . However, not until the discovery(105) of “honest” stripe-ordered phases in the closely related compound  $\text{La}_{1.6-x}\text{Nd}_{0.4}\text{Sr}_x\text{CuO}_4$  was the interpretation of these peaks as being due to stripe fluctuations made unambiguously clear. For instance, as shown in Fig. 7, the magnetic structure factor at low temperature and small but finite frequency,  $\hbar\omega = 3$  meV,

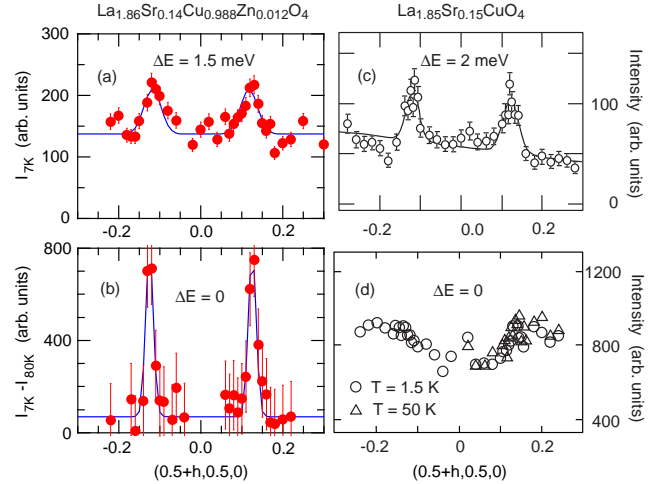


FIG. 8 Comparison of magnetic scattering measurements in  $\text{La}_{2-x}\text{Sr}_x\text{CuO}_4$  with and without Zn; all scans are along  $Q = (\frac{1}{2} + h, \frac{1}{2}, 0)$ , measured in reciprocal lattice units. (a) Scan at  $E = 1.5$  meV and  $T = 7$  K, and (b) difference between elastic scans measure at 7 K and 80 K, both for  $\text{La}_{1.86}\text{Sr}_{0.14}\text{Cu}_{0.988}\text{Zn}_{0.012}\text{O}_4$  ( $T_c = 19$  K).(113) (c) Scan at  $E = 2$  meV and  $T = 38$  K (Ref. 114), and (d) elastic scans at  $T = 1.5$  K (circles) and 50 K (triangles),(86) for  $\text{La}_{1.85}\text{Sr}_{0.15}\text{CuO}_4$  ( $T_c = 38$  K). Measurement conditions were different for each panel; see references for details.

looks very similar (in absolute magnitude and width) both  $\text{La}_{1.6-x}\text{Nd}_{0.4}\text{Sr}_x\text{CuO}_4$  with  $x = 0.12$ , where elastic scattering indicating static ordered stripes has been detected,(105) and in  $\text{La}_{2-x}\text{Sr}_x\text{CuO}_4$  with  $x = 0.15$ , where no such static order is discernible.(106) As discussed in the previous section, this is precisely the expected(49) behavior near a quantum critical point, where presumably the partial substitution of La by Nd has moved the system from slightly on the quantum disordered to slightly on the ordered side of a stripe ordering quantum critical point.(107) We can now confidently characterize  $\text{La}_{2-x}\text{Sr}_x\text{CuO}_4$  over an extremely broad range of doping as either being in a stripe-ordered, or a nearly ordered stripe-liquid phase.

An important test of this idea comes from studies of the changes in  $S(\mathbf{k}, \omega)$  produced by weak disorder. Specifically, in Fig. 8, we compare the low frequency(108) and elastic(109) pieces of the magnetic structure factor of  $\text{La}_{2-x}\text{Sr}_x\text{CuO}_4$  in the presence and absence of a small concentration (1.2%) of Zn impurities. (Zn substitutes for Cu.) As one might have expected, the Zn slightly broadens the  $\mathbf{k}$  space structure, although not enormously.(86; 110) Most dramatically, the Zn “pins” the stripe fluctuations, in the sense that what appears only as finite frequency fluctuation effects in the Zn free material, is pushed to lower frequencies and even to  $\omega = 0$  by the quenched disorder(111).

The issue still remains actively debated whether or not various fluctuation effects seen in neutron scattering studies of the other widely studied families of high tem-

perature superconductors, especially  $\text{YBa}_2\text{Cu}_3\text{O}_{6+y}$  and  $\text{Bi}_2\text{Sr}_2\text{CaCu}_2\text{O}_{8+\delta}$ , can be associated with stripe fluctuations. We will not review this debate here, but will touch on it again in Secs. V.B and V.C, below.

One question arises (115) concerning how we can distinguish a fluctuating stripe phase from a fluctuating checkerboard phase, which breaks translation symmetry but preserves the symmetry under exchange of  $x$  and  $y$ ? Of course, the strongest indication that stripes, rather than checkerboards are responsible for the observed fluctuations comes from the presence of “nearby” stripe-ordered phases, and the absence of any clear evidence of actual ordered checkerboard phases in any doped antiferromagnet, to date. However, in theoretical studies(116) both types of order appear to be close to each other in energy, so this argument should not be given undue weight.

Where both spin and charge peaks are observed, it turns out that there is a straightforward way to distinguish. From Landau theory, it follows (42) that there is a preferred relation between the spin and charge ordering wave-vectors,  $\mathbf{Q}_s + \mathbf{Q}'_s = \mathbf{Q}_{ch}$ . For stripe order, this means that the spin and charge wave-vectors are parallel to each other, and related (up to a reciprocal lattice vector) by the relation  $2\mathbf{Q}_s = \mathbf{Q}_{ch}$ . However, in the case of checkerboard order, the dominant spin ordering wave-vector is *not* parallel to the charge ordering wave vectors; if  $\mathbf{Q}_{ch} = \pm\delta_{ch}\hat{\mathbf{e}}_x$  and  $\mathbf{Q}'_{ch} = \pm\delta_{ch}\hat{\mathbf{e}}_y$ , the corresponding spin ordering vectors,  $\mathbf{Q}_s = \pi \pm (1/2)\delta_{ch}[\hat{\mathbf{e}}_x + \hat{\mathbf{e}}_y]$  and  $\mathbf{Q}'_s = \pi \pm (1/2)\delta_{ch}[\hat{\mathbf{e}}_x - \hat{\mathbf{e}}_y]$  satisfy the requisite identities. Thus, the relative orientation of the spin and charge peaks can be used to distinguish fluctuating stripe order from fluctuating checkerboard order.(110)

## B. STM measurements and stripes

STM is a static probe and thus cannot detect any structure associated with fluctuating order unless something pins it.(38; 117; 118; 119; 120; 121; 122; 123; 124; 125) Density or “Friedel oscillations” (126) in simple metals produced by the presence of a defect are directly related to Fermi-surface-derived non-analyticities in the susceptibility,  $\chi(\mathbf{k})$ . However, “generalized Friedel oscillations” can occur in more diverse systems in which the relevant structure in  $\chi(\mathbf{k})$  is not directly related to any feature of a Fermi surface. For instance, a bosonic superfluid on a lattice close to a second order transition to an insulating, bosonic crystalline phase would exhibit generalized Friedel oscillations with the characteristic wave length of the roton-minimum—these oscillations, in a very direct sense, would image the fluctuating crystalline order present in the fluid state.

There are a few important features of generalized Friedel oscillations which follow from general principles. If the liquid state is proximate to a highly anisotropic state, such as a stripe state, the values of  $\mathbf{k} = \mathbf{Q}$  at which  $\chi$  has maxima will reflect the pattern of spatial symmetry breaking of the ordered state, but  $\chi(\mathbf{k})$  will

respect the full point-group symmetry of the crystal unless the liquid state spontaneously breaks this symmetry, *e.g.* is a nematic. So, the generalized Friedel oscillations around a point impurity in a stripe liquid phase will inevitably form a checker-board pattern, unless some form of external symmetry breaking field is applied (72). Distinguishing “just Friedel oscillations” from “generalized Friedel oscillations” may not always be straightforward, as discussed in Secs. III and IV.

There is another form of spatial modulation of the density of states, one with a period which disperses as a function of the probe energy, which is sometimes (incorrectly, we believe) referred to in the STM literature as Friedel oscillations. This latter effect, which was first demonstrated by Cromie *et al.* (127), is produced by the elastic scattering of quasiparticles of given energy off an impurity. The resulting interference between scattered waves leads to variations of the local density of states at wave vectors  $\mathbf{Q} = \mathbf{k} - \mathbf{k}'$ , where  $\mathbf{k}$  and  $\mathbf{k}'$  are the wave-vectors of states with energy  $E = \epsilon(\mathbf{k}) = \epsilon(\mathbf{k}')$ , as determined by the band-structure,  $\epsilon(\mathbf{k})$ . Generalized versions of these oscillations can occur even when there are no well defined quasi-particles, so long as there are some elementary excitations of the system with a well-defined dispersion relation, as is shown in Sec. III.

Modulations which reflect the spectrum of elementary excitations are distinguishable(128) from those related to incipient order in a variety of ways: Whereas incipient order produces effects peaked at isolated ordering vectors,  $\mathbf{Q}$ , independent of energy, the single particle effects are peaked along extremal curves in  $\mathbf{k}$  space which disperse as a function of  $E$ . Peaks in the Fourier transformed LDOS,  $N(\mathbf{k}, E)$ , produced by incipient order tend to be phase coherent while other features either have a random phase, or a phase that is strongly energy dependent. Indeed, the phase information may be the best way to distinguish the consequences of incipient order from interference effects.

To demonstrate the effect of the phase, assume we have measured  $N_L(\mathbf{r}, \mathbf{E})$  the LDOS at a particular bias voltage,  $V = E/e$ , on a sample of size  $L \times L$ . Its Fourier transform,  $N_L(\mathbf{k}, E)$ , has an arbitrary  $\mathbf{k}$ -dependent but  $E$ -independent phase,  $e^{-i\mathbf{k} \cdot \mathbf{r}_0}$ , which depends on the choice of origin of coordinates,  $\mathbf{r}_0$ . As discussed above,  $N_L(\mathbf{k}, E)$  can be expected to have contributions from incipient order (with wave vector  $\mathbf{Q}$ ), dispersing quasi-particles, and noise. Integrating the signal over a finite energy window yields the quantity  $\tilde{N}(\mathbf{k}, E)$ , in which the contributions from incipient order from the entire range of integration add constructively, while other features tend to interfere destructively. This mode of analysis is particularly useful if an energy window can be found in which none of the dispersing features expected on the basis of band-structure considerations have wave vectors equal to the expected ordering wave vector,  $\mathbf{Q}$ . (A complementary mode of analysis, which emphasizes the dispersing features of the data, is discussed in Sec. IV.)

Indeed, Howald *et al.* have already demonstrated the first half of this point (39) in STM studies of a very

slightly overdoped sample of  $\text{Bi}_2\text{Sr}_2\text{CaCu}_2\text{O}_{8+\delta}$  ( $T_c = 86$ ). They identified a non-dispersing peak in  $N(\mathbf{k}, E)$  at  $\mathbf{k} = \pm \mathbf{Q}_{\text{ch}} \approx \pm(2\pi/a)(0.25, 0)$  and  $\mathbf{k} = \pm \mathcal{R}[\mathbf{Q}_{\text{ch}}] = \pm(2\pi/a)(0, 0.25)$  (see Fig. 9), and showed that at these wave numbers, the Fourier transform of the phase of  $N(\mathbf{k}, E)$  is energy independent for  $E$  between 0 and 40 meV, at which point the amplitude crosses through zero—*i.e.*, the sign of the signal changes. The constancy of the phase implies that the location in real-space of the density of states modulation is fixed at all energies, which strongly indicates that it reflects pinned incipient order.

However, as explained above, the existence of incipient order can be magnified if we integrate the LDOS as a function of energy. In Fig. 9(a) we show data from Howald *et al.* (39; 120) in which the values of  $dI/dV \propto N_L(\mathbf{k}, E)$  were obtained by a Fourier transform of a real space image at various voltages,  $V = E/e$ , on a patch of surface of size  $L = 160\text{\AA}$ . Here,  $\mathbf{k}$  is taken to lie along the  $\langle 1, 0 \rangle$  direction. In Fig. 9b, we show the same data integrated over energy from 0 to  $E$ ,  $I/V \propto \tilde{N}_L(\mathbf{k}, E)$ . It is apparent that integration enhances the strength of the peak at  $\mathbf{Q}_{\text{ch}}$ , and depresses the remaining signal, especially when  $E$  is smaller than the maximum superconducting gap value,  $\Delta_0 \approx 35$  meV.

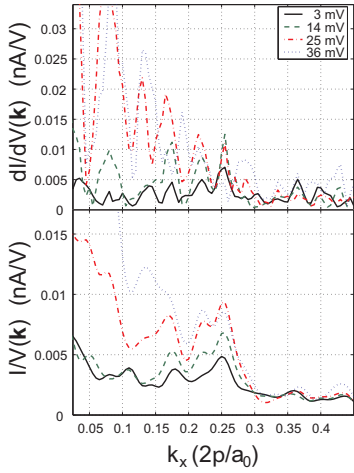


FIG. 9 The Fourier transform of the local density of states from an STM study of a near optimally doped crystal of  $\text{Bi}_2\text{Sr}_2\text{CaCu}_2\text{O}_{8+\delta}$ .  $\mathbf{k}$  is taken along the  $\langle 1, 0 \rangle$  direction, in a tetragonal convention. a) shows  $dI/dV \propto N(\mathbf{k}, E)$  measured at fixed voltage,  $V = E/e$ . b) shows  $I/V \propto \tilde{N}(\mathbf{k}, E)$ , which is the integral of the quantity shown in a) from  $V = 0$  to  $V = E/e$ .

A similar analysis of the energy integrated quantity,  $\tilde{N}(\mathbf{k}, E = 12 \text{ meV})$ , was adopted previously by Hoffman *et al* (38) in their STM experiments on density of states oscillations associated with vortex cores in the superconducting state of similar materials. Very large amplitude oscillations (much larger than the disorder induced signal

discussed until now) were observed with the same characteristic wave vector,  $\mathbf{k} = \mathbf{Q}_{\text{ch}}$ . We consider this to be the most direct evidence to date of incipient stripe order in optimally doped  $\text{Bi}_2\text{Sr}_2\text{CaCu}_2\text{O}_{8+\delta}$ .

## 1. Concerning differing interpretations of the STM spectra

As mentioned in the introduction, there is controversy in the literature concerning the interpretation of the STM spectra, although there seems to be no disagreement concerning the data itself. Specifically, Hoffman *et. al.*(37) have recently suggested that there is no need to invoke incipient stripe order to interpret any of the STM spectra. While it is certainly true(37; 68) that much of the observed STM spectrum comes from dispersive features associated with the elementary excitations of the system (although these are almost certainly(129; 131) not, for the most part(132), well defined quasiparticles), we feel that when the data are analyzed as in Fig. 9, it demonstrates that interference effects cannot account for the behavior of the low energy part of the spectrum. However, since this point is important and disputed, it is worth examining in a bit more depth.

The failure of interference effects to account for the observed low energy spectra is particularly clear, in our opinion, given the “band structure” that has been deduced(133; 134) from ARPES experiments. It turns out that the  $\mathbf{k}$  dependence of the electron spectral function measured by ARPES can be well approximated by a phenomenological quasiparticle band structure. Using this band structure(133), one can readily compute the expected(68; 71; 135) interference effects due to quasiparticles with energies  $E_{\mathbf{k}} = \sqrt{\Delta_{\mathbf{k}}^2 + \epsilon_{\mathbf{k}}^2}$ , where  $\Delta_{\mathbf{k}} = \frac{\Delta_0}{2}[\cos(k_x a) - \cos(k_y a)]$  is the d-wave superconducting gap and  $\epsilon_{\mathbf{k}}$  is the normal-state quasiparticle dispersion measured from the Fermi energy (*i. e.*,  $\epsilon_{\mathbf{k}} = 0$  on the Fermi surface). If we consider the interference signal as a function of voltage at fixed wave vector,  $\mathbf{Q} = (2\pi/a)\langle 0.25, 0 \rangle$ , we are most sensitive to the scattering between pairs of degenerate states, *i. e.* states with  $\mathbf{Q} = \mathbf{k}' - \mathbf{k}$  and  $eV = E_{\mathbf{k}} = E_{\mathbf{k}'}$ . The minimum voltage at which this resonance condition can be satisfied is achieved when the states in question are on the Fermi surface, consequently their energy is determined by the superconducting gap. Specifically, this implies that  $\mathbf{k} = (\pi/a)(0.25, k_y)$ , and  $\mathbf{k}' = (\pi/a)(-0.25, k_y)$ , where  $k_y \approx 0.6$  is determined directly from the measured(136; 137; 138) location of the Fermi surface. This gives an estimate of the lowest energy for quasiparticle scattering of  $\sim \Delta_0/2 \sim 15\text{--}20$  meV. (The gap observed in ARPES experiments is  $\Delta_0 \sim 30\text{--}40$  meV (139; 140; 141).) What this means is that no peak structure in  $N(\mathbf{k}, E)$  at energies  $E \leq 15$  meV can be attributed to quasiparticle interference effects! In this context, particular attention should be paid to the peak at  $\mathbf{k} = \mathbf{Q}_{\text{ch}}$  seen in the curves in Fig. 9 with  $E \leq 15$  meV, and to the peaks observed by Hoffman *et. al.* (38) be-

low 12 meV in vortex core halos. The absence of low energy peaks in the interference signal at the stripe ordering vector can be verified by comparison with explicit microscopic calculations; for instance,  $N(\mathbf{k}, \mathbf{E})$  was recently computed by Polkovnikov *et. al.* (135) for non-interacting quasi-particles scattering from a point impurity; it is apparent from their Fig. 4 that, at energies of 20 meV and below, there is a local *minimum* in the neighborhood of  $\mathbf{k} = \mathbf{Q}_{\text{ch}}$ !

One further feature of all the data that has been reported to date is worth commenting on—this is the large (factors of 2 or 3) differences that are observed(37) in the peak intensities at  $\mathbf{Q}_{\text{ch}}$  and  $R[\mathbf{Q}_{\text{ch}}]$ . Systematic experiments have not, yet, been conducted to verify whether this effect is real, or an experimental artifact. If it is not an artifact, then this observation is among the first microscopic pieces of evidence of a strong local tendency to stripe orientational (*i.e.* nematic) order. In addition, such large anisotropies are something that cannot be accounted for in any simple way by quasi-particle interference (nor local checkerboard order). It is important to bear in mind, however, that even if the observed anisotropy reflects nematic order, it is expected to decrease in magnitude(39) in direct proportion to  $A^{-1/2}$ , where  $A$  is the area of the field of view, due to the unavoidable domain structure produced by quenched disorder. In any case, this is an extremely interesting feature of the data to pursue.

### C. Detecting Nematic Order

While stripe order necessarily implies nematic order, the converse is not true. Although nematic order involves the spontaneous breaking of a spatial (point-group) symmetry, when there is no accompanying breaking of translation symmetry, even the identification of the ordered state is somewhat subtle, and this holds doubly for fluctuation effects. Moreover, since quenched disorder is always relevant and results in domain structure, true macroscopic measurements of spontaneous nematic symmetry breaking are not possible. The difficulty of detecting the rotational-symmetry breaking associated with ordered stripes is illustrated by the case of  $\text{La}_{2-x}\text{Sr}_x\text{NiO}_{4+\delta}$ , a non-superconducting structural analogue of  $\text{La}_{2-x}\text{Sr}_x\text{CuO}_4$ . Even transmission electron microscopy, which is capable of measuring over a fairly small sample area, tends to yield superlattice diffraction peaks for stripe order that reflect the 4-fold symmetry of the  $\text{NiO}_2$  planes in the tetragonal crystal structure.(142) Only recently have electron diffraction patterns consistent with the 2-fold symmetry of an ordered stripe domain been reported.(143) Thus, almost all tests of nematic order in solids necessarily involve the observation of an unreasonably large, and strongly temperature dependent anisotropy in the electronic response to a small symmetry breaking field which favors the  $x$  direction over the  $y$  direction.

### 1. Transport Anisotropies

An example of a system in which this approach has been successfully applied is provided by the 2DEG in quantum Hall devices. While the fractional quantum Hall effect dominates the physics at very high magnetic fields, at intermediate magnetic fields (so that more than one Landau level is occupied), it has recently been discovered (79) that there are a set of anisotropic states which have been identified (144; 145) as being quantum Hall nematics, and which can be thought of as melted versions of the long predicted (146) quantum Hall smectic (or stripe) phases. These phases are characterized by a large resistance anisotropy,  $\rho_{xx} \gg \rho_{yy}$ , which onsets very strongly below a characteristic temperature,  $T_n \sim 100$  mK. The precise origin of the symmetry breaking field which aligns the nematic domains in these experiments has not been unambiguously determined.(147) However, by applying (145; 148) an in-plane magnetic field, the magnitude of the symmetry breaking field can be varied, and the transition can be significantly rounded (giving evidence (145) that local stripe order persists up to temperatures well in excess of  $T_n$ ), and even the orientation of the nematic order can be switched, resulting in a state with  $\rho_{xx} \ll \rho_{yy}$ .

Experiments that involve such fine control of an external symmetry-breaking field are considerably harder to carry out in the context of the cuprates. Some of the relevant materials, such as  $\text{Bi}_2\text{Sr}_2\text{CaCu}_2\text{O}_{8+\delta}$  and  $\text{La}_{2-x}\text{Sr}_x\text{CuO}_4$  with  $x > 0.05$ , have an orthorhombic axis at  $45^\circ$  to the expected stripe directions (*i.e.*, a nematic phase can be defined in terms of spontaneous breaking of the mirror plane which lies along the orthorhombic  $a$ -axis.) In these materials, if one wishes to align the nematic domains, one must apply a suitable external symmetry-breaking field such as a uniaxial strain or in-plane magnetic field; however, such experiments tend to be challenging.

When the principle axes of an orthorhombic phase lie parallel to the expected stripe directions, the orthorhombicity (typically  $< 2\%$  in cuprates) plays the role of a small, external symmetry-breaking field. Examples where this occurs are superconducting  $\text{YBa}_2\text{Cu}_3\text{O}_{6+y}$  with  $0.35 \leq y \leq 1$  and non-superconducting  $\text{La}_{2-x}\text{Sr}_x\text{CuO}_4$  with  $0.02 \leq x < 0.05$ . In both of these cases, resistivity anisotropies as large as a factor of 2 have been observed(80) in detwinned single crystals. Moreover, as in the quantum Hall case, this anisotropy is strongly temperature dependent; in  $\text{La}_{2-x}\text{Sr}_x\text{CuO}_4$ ,  $|\rho_{aa}/\rho_{bb} - 1| < 10\%$  for temperatures in excess of  $T_n \sim 150$  K. Polarization dependent measurements of the infra-red conductivity on a detwinned  $x = 0.03$  crystal of  $\text{La}_{2-x}\text{Sr}_x\text{CuO}_4$  reveal that the frequency dependence of the conductivity anisotropy has a scale comparable to  $kT_n$ .(149) Large anisotropies in the frequency-dependent conductivity have also been observed(150) in  $\text{YBa}_2\text{Cu}_3\text{O}_{6+y}$  and in  $\text{YBa}_2\text{Cu}_4\text{O}_8$ , although in those cases, some part of the conductivity anisotropy must be due directly to the Cu-O chains. Taken together, these

various observations are circumstantial evidence of a fair degree of local stripe order, and of the presence of a nematic phase—the trouble being that, without a somewhat quantitative theory (which does not exist), it is hard to say how large an observed resistance anisotropy must be to be accepted as being an “unreasonably large” response to the orthorhombicity, that is, one that can only be understood in terms of the alignment of nematic domains.

More subtle investigations of orientational symmetry breaking can be undertaken by studying the transport in the presence of a magnetic field. A very clever approach along these lines was introduced by Noda, Eisaki, and Uchida(151). They applied a voltage along one axis of the  $\text{CuO}_2$  planes and a magnetic field perpendicular to the planes in order to break the 4-fold symmetry of the crystal structure and to obtain evidence of one-dimensional charge transport. In a stripe-ordered state, the geometry used should be sensitive primarily to those domains in which the stripes are aligned parallel to the direction of the applied voltage. For  $x \leq \frac{1}{8}$ , they found that, within the stripe-ordered phase, the transverse conductivity tends to zero at low temperature while the longitudinal conductivity remains finite. (This effect has been explained in terms of the electron-hole symmetry of a  $\frac{1}{4}$ -filled charge stripe.(152; 153))

Ando and collaborators(154) have observed a remarkable anisotropy of the resistivity tensor induced by an in-plane magnetic field in non-superconducting  $\text{YBa}_2\text{Cu}_3\text{O}_{6+y}$  with  $y = 0.32$  and  $y = 0.3$ . (Presumably, these samples are antiferromagnetic.) The results were interpreted as evidence for nematic stripe order. Alternative explanations in terms of anisotropy associated with spin-orbit coupling in the antiferromagnetic phase have also been proposed.(155; 156) This example illustrates the difficulty in making a unique association between a bulk anisotropy and microscopic stripe order.

Finally, we note that there is a very direct way to detect nematic order using light scattering. This approach is well known from studies of classical nematic liquid crystals (157). Recently Rüthausen and coworkers (158) have used light scattering techniques to study the behavior of the low-frequency dielectric tensor of the manganite  $\text{Bi}_{1-x}\text{Ca}_x\text{MnO}_3$  near and below the charge-ordering transition at  $T_{co} \sim 160\text{K}$ . In these experiments, a pronounced anisotropy of the dielectric tensor was found with a sharp temperature-dependence near  $T_{co}$ . Raman scattering studies by the same group show that long range positional stripe order sets in only at much lower temperatures. These experiments suggest that this manganite is in a nematic state below the transition at  $T_{co}$ , and long range charge stripe order occurs at much lower temperatures.

## 2. Anisotropic Diffraction Patterns

A more microscopic approach is to directly measure the nematic order parameter,  $Q_{\mathbf{k}}$  of Eq. (2.1), by diffraction. This was done (more or less) by Mook *et al.*(159), in neutron scattering studies of the magnetic dynamic structure factor of a partially (2 to 1) detwinned sample of  $\text{YBa}_2\text{Cu}_3\text{O}_{6+y}$  with  $y = 0.6$  and  $T_c \approx 60\text{ K}$ . No elastic scattering corresponding to actual stripe order was detected; however, well developed structure was observed in the inelastic spectrum at the two-dimensional wave vectors  $\mathbf{Q}_s \approx (0.5 \pm 0.1, 0.5)$  and  $\mathbf{Q}'_s \approx (0.5, 0.5 \pm 0.1)$  in units of  $2\pi/a$ . Remarkably, the intensities of the peaks at  $\mathbf{Q}_s$  were found to be about a factor of 2 larger than those of the  $\mathbf{Q}'_s$  peaks, consistent with the supposition that, in a single twin domain, the incommensurate inelastic structure is entirely associated with ordering vectors perpendicular to the chain direction, *i.e.*  $Q_{\mathbf{Q}} \approx 1$ .

Although the presence of chains in this material certainly means that there is no symmetry operation that interchanges the  $a$  and  $b$  axes, the copper-oxide planes are nearly tetragonal. Thus, it seems to us that the extreme anisotropy of the inelastic scattering is very strong evidence of a nematic liquid phase in this material. As pointed out by Mook *et al.*(159) this conclusion also offers a potential explanation for the observed(150) large but nearly temperature independent superfluid anisotropy in the  $a$ - $b$  plane. We have not found any published data on the temperature dependence of  $Q_{\mathbf{Q}_{ch}}$ ; the identification of a characteristic temperature,  $T_n$ , above which the anisotropy decreases substantially from its low temperature value would go a long way toward confirming that the superfluid anisotropy is a collective effect, and not a straightforward consequence of the presence of chains in the crystal.

Interesting anisotropies have also been observed in optical phonon branches of  $\text{YBa}_2\text{Cu}_3\text{O}_{6+y}$  with  $y = 0.6$ . The identification by Mook *et al.*(159) of an anomalous broadening of a bond-bending mode at a wave vector expected for charge-stripe order is potentially the most direct evidence of nematic order. However, conflicting results have been reported by Pintschovius *et al.*(160), who have instead observed a zone-boundary softening of the bond-stretching mode propagating along  $\mathbf{b}$  but not for that along  $\mathbf{a}$ . This latter anisotropy is unlikely to be directly associated with a stripe modulation wave vector since the anomaly occurs along the direction parallel to the Cu-O chains. Of course, this does not necessarily rule out a connection with stripes, as the softening might be associated with anisotropic screening due to charge fluctuations along the stripes.

In an attempt to understand the effects of stripe order on phonons, a neutron scattering study(161) was recently performed on  $\text{La}_{1.69}\text{Sr}_{0.31}\text{NiO}_4$ . Although the charge-ordering wave vector did not play an obvious role, the high-energy bond-stretching mode propagating parallel (and perpendicular) to the stripe modulation exhibited an energy splitting toward the zone boundary, while

along the Ni-O bond direction (at 45° to the stripes) a softening from zone center to zone boundary was observed with a magnitude similar to that in the cuprates. A better understanding of the nature of the relevant electron-phonon coupling processes is required to make progress here.

### 3. STM Imaging of Nematic Order

Because it is a local but spatially resolved probe, STM is actually the optimal probe of nematic order. One way it can be used, which is illustrated in Fig. 10, has been explored by Howald *et al.* (39; 120) What is shown here is a filtered version of  $N(\mathbf{r}, E)$  measured on a patch of surface of a very slightly overdoped crystal of  $\text{Bi}_2\text{Sr}_2\text{CaCu}_2\text{O}_{8+\delta}$  ( $T_c = 86$  K). Specifically, Howald *et al.* defined a filtered image

$$N_f(\mathbf{r}, E) = \int d\mathbf{r}' f(\mathbf{r} - \mathbf{r}') N(\mathbf{r}', E) \quad (5.1)$$

where in the present case, the filter function,  $f$ , has been defined so as to accentuate the portions of the signal associated with stripe order

$$f(\mathbf{r}) \propto \Lambda^2 e^{-r^2 \Lambda^2/2} [\cos(\pi x/2a) + \cos(\pi y/2a)]. \quad (5.2)$$

Clearly,  $f(\mathbf{r}) \rightarrow \delta(\mathbf{r})$  when  $\Lambda \rightarrow \infty$ , while  $N_f = N(\mathbf{Q}_{\text{ch}}, E) + N(\mathcal{R}[\mathbf{Q}_{\text{ch}}], E) + \text{c.c.}$  in the limit  $\Lambda \rightarrow 0$ . For intermediate values of  $\Lambda$ , the filtered image shows only that portion of the signal we have associated with pinned stripes. The roughly periodic structure in the image has period  $4a$ —we know independently from the analysis in Section V.B that there is prominent structure in the raw data with this period, but even were there not, the filtering would build in such structure. However, what is clear from the image is that there is a characteristic domain structure, within which the stripes appear to dominantly lie in one direction or the other. The domain size is seen to be on the order of  $100 \text{ \AA} \sim 25a$ , which is large compared to  $\Lambda^{-1}$  and, more importantly, roughly independent (120) of the precise value of  $\Lambda$ . This domain size is a characteristic correlation length of the pinned nematic order.

This particular method of analysis builds directly on the realization of the nematic as a melted stripe ordered state. Indeed, looking at the figure, one can clearly identify dislocations and disclinations in what looks like a fairly well developed locally ordered stripe array.

More generally, STM could be used to directly measure the two independent components of a suitably defined traceless symmetric tensor density. The simplest such quantities are

$$\begin{aligned} \mathcal{Q}(\mathbf{r}, E) &= [\partial_x^2 - \partial_y^2] N(\mathbf{r}, E) \\ \mathcal{Q}'(\mathbf{r}, E) &= \partial_x \partial_y N(\mathbf{r}, E) \end{aligned} \quad (5.3)$$

Of course, these quantities, like the local density of states itself, will typically have features which reflect the inter-

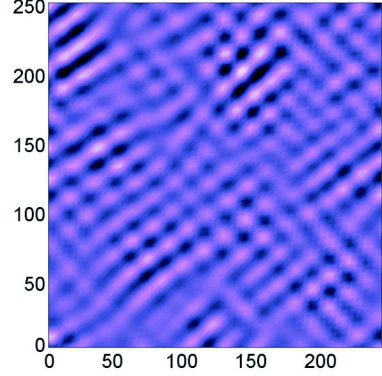


FIG. 10 A filtered version of the local density of states map,  $N_f(\mathbf{r}, E)$ , of the local density of states on a surface patch of a  $\text{Bi}_2\text{Sr}_2\text{CaCu}_2\text{O}_{8+\delta}$  crystal. Here,  $E = 15$  meV and the distances on the  $x$  and  $y$  axes are measured in angstroms. The filter is defined in Eq. (5.1) with  $\Lambda = (2\pi/15a)$ .

ference between elementary excitations, and other extraneous information. To obtain a better view of the long wave-length nematic correlations, we should again integrate these densities over a suitable energy interval,  $\Omega$ , and filter out the short wavelength components:

$$\tilde{\mathcal{Q}}_f(\mathbf{r}) = \int_0^\Omega \frac{dE}{\Omega} \int d\mathbf{r}' f(\mathbf{r} - \mathbf{r}') \mathcal{Q}(\mathbf{r}', E) \quad (5.4)$$

where  $f$  might be a Gaussian filter, as in Eq. (5.2), but without the cosine factors. A map of  $\tilde{\mathcal{Q}}_f$  should produce a domain structure, similar to that shown in Fig. 10, but without all the short wavelength detail. Where the domain size,  $L_N$ , is large compared to  $a$ , the resulting picture should look qualitatively the same independent of the range over which the signal is coarse-grained, so long as  $L_N \gg \Lambda^{-1} \gg a$ . The above procedure should work well if there are no other long-wavelength features in the data. Unfortunately, for BSCCO, the inhomogeneities in the gap structure (39; 122) hamper such a procedure.

### D. “1/8” Anomaly

Many members of the lanthanum cuprate family of high-temperature superconductors exhibit strong singularities in the doping dependence of various interesting low-temperature properties at  $x = 1/8$ ; together, these phenomena are referred to as the “1/8 anomaly.” For instance, in  $\text{La}_{2-x}\text{Ba}_x\text{CuO}_4$  and  $\text{La}_{1.6-x}\text{Nd}_{0.4}\text{Sr}_x\text{CuO}_4$ , there is (162; 163) a deep minimum in  $T_c(x)$ ; in  $\text{La}_{2-x}\text{Ba}_x\text{CuO}_4$  and  $\text{La}_{2-x}\text{Sr}_x\text{CuO}_4$  there is a pronounced (164; 165) maximum in  $\alpha(x)$ , the isotope exponent  $\alpha \equiv d\log(T_c)/d\log(M)$ ; and in  $\text{La}_{2-x}\text{Sr}_x\text{CuO}_4$  there is a pronounced (166) minimum in the superfluid density,  $n_s(x)$ . One of the central infer-

ences drawn by Tranquada *et al.*(105) following the discovery of stripe order in  $\text{La}_{1.6-x}\text{Nd}_{0.4}\text{Sr}_x\text{CuO}_4$  is that this 1/8 anomaly is associated with a commensurate lock-in of the stripe structure—at  $x = 1/8$  the preferred spacing between charge stripes is 4 lattice constants, so there is an additional commensuration energy which stabilizes stripe order at this particular hole density.

While it is possible to imagine other forms of CDW order which would similarly be stabilized at  $x = 1/8$ , there can be no doubt that in this family of materials the 1/8 effect is associated with stripe order. This has been confirmed, for example, in  $\text{La}_{2-x}\text{Sr}_x\text{CuO}_4$  where quasi-elastic magnetic scattering from spin-stripe order has been detected(85; 86) for  $x$  in the neighborhood of 1/8; in low-energy inelastic measurements, Yamada *et al.*(114) have shown that the magnetic peak width is most narrow at  $x = 1/8$ . Correspondingly, slow (probably glassy) spin fluctuations have been detected by  $\mu\text{SR}$  in the same material with a somewhat arbitrarily defined onset temperature,  $T_g(x)$ , which has(166) a pronounced peak at  $x = 1/8$ . The fact that quasi-elastic magnetic order as detected by neutron scattering onsets at a considerably higher temperature than that detected by  $\mu\text{Sr}$  is clearly a consequence of the inevitable glassiness of a density-wave transition in the presence of quenched disorder; it reflects the differences in the time scales of the two probes, not the presence of two distinct ordering phenomena. More recently, new experiments on  $\text{La}_{2-x}\text{Sr}_x\text{CuO}_4$  as a function of  $x$  show pronounced singularities in the  $x$  dependence of the  $c$ -axis Josephson plasma edge(149) and in the low temperature thermal conductivity(167); these effects can be interpreted straightforwardly in terms of a peak in the stability of the charge-stripe order at  $x = 1/8$ . Furthermore, charge-stripe order has now been detected directly by neutron diffraction(84) in  $\text{La}_{1.875}\text{Ba}_{0.125-x}\text{Sr}_x\text{CuO}_4$ .

The large drop in  $T_c$  at  $x = 1/8$  found in  $\text{La}_{2-x}\text{Ba}_x\text{CuO}_4$  is not observed in  $\text{La}_{2-x}\text{Sr}_x\text{CuO}_4$ ; however, such a dip in the doping dependence of  $T_c$  can be induced in  $\text{La}_{2-x}\text{Sr}_x\text{CuO}_4$  (centered at  $x = 0.115$ ) by substitution of 1% Zn for Cu, as shown some time ago by Koike *et al.*(168) Zn substitution enhances local magnetic order at low temperature near the dip minimum, as detected by  $\mu\text{SR}$ .(166; 169) Given the clear association between the 1/8 anomaly and stripe order in  $\text{La}_{2-x}\text{Sr}_x\text{CuO}_4$ , an indirect method to look for the presence of local stripe order in other families of cuprate superconductors is to test whether a 1/8 anomaly can be induced by Zn substitution. In the case of  $\text{YBa}_2\text{Cu}_3\text{O}_{6+y}$ , there already exists in the literature strong evidence from the work of Tallon and collaborators (170) that the “60-K plateau” in the  $y$  dependence of  $T_c$  is not, primarily, a reflection of some form of oxygen ordering in the chain layers, as is commonly assumed, but is rather a barely resolved 1/8 anomaly; this conclusion is also supported by a Ca-substitution study(171) and by a recent study of transport properties.(172) To further test this idea, Koike and collaborators(171; 173; 174)

studied the doping dependence of  $T_c$ , and of  $T_g$  measured by  $\mu\text{SR}$ , in lightly Zn doped  $\text{YBa}_2\text{Cu}_3\text{O}_{6+y}$  and  $\text{Bi}_2\text{Sr}_2\text{CaCu}_2\text{O}_{8+\delta}$ . They have found that there is some tendency for light Zn doping to produce a dip in  $T_c(x)$  and a more impressive peak in  $T_g(x)$  at  $x \approx 1/8$  in both  $\text{YBa}_2\text{Cu}_3\text{O}_{6+y}$  and  $\text{Bi}_2\text{Sr}_2\text{CaCu}_2\text{O}_{8+\delta}$ . Related results have been reported(175; 176) for the single-layer system  $\text{Bi}_{2-x}\text{Sr}_{2-x}\text{La}_x\text{CuO}_{6+\delta}$ . While it is clear that more work is needed to test the connection between the “1/8 anomaly” and stripe pinning in these various systems, we consider this a promising approach to the problem, as it permits evidence of local order to be obtained using a variety of probes which can be applied in materials for which large crystals, and/or easily cleaved surfaces are not easily obtained.

## E. Other Probes

It is clear that the most direct evidence for stripes comes from techniques that can provide images of charge, spin, and/or lattice modulations in real space (STM) or in reciprocal space (diffraction techniques). We have already discussed neutron and X-ray diffraction, but explicit mention should also be made of transmission electron microscopy (TEM). The charge stripes in  $\text{La}_{2-x}\text{Sr}_x\text{NiO}_{4+\delta}$  were first detected by TEM,(142) and a recent study has provided high-resolution TEM images of local stripe order in  $\text{La}_{1.725}\text{Sr}_{0.275}\text{NiO}_4$ .(143) So far, TEM studies have not provided positive evidence for stripes in any cuprates, but, though challenging, it should be possible to do so.

Less direct but extremely valuable information comes from techniques that are sensitive to local order. We have already mentioned evidence for local, static hyperfine fields and slowly fluctuating hyperfine fields obtained by  $\mu\text{SR}$ . Besides providing a practical measure of local magnetic order as a function of doping,(87; 177)  $\mu\text{SR}$  can detect the distribution of local hyperfine fields in a sample with relatively uniform order,(178) as well as being able to detect inhomogeneous magnetic or superconducting order.(179) Related information can be obtained by NMR and NQR techniques, where the latter also provides information on the distribution of local electric-field gradients. Some of the first evidence for spatial inhomogeneity of magnetism in lightly-doped  $\text{La}_{2-x}\text{Sr}_x\text{CuO}_4$ , consistent with stripe-like behavior, was obtained in a La NQR experiment by Cho *et al.*(180) Later experiments(181; 182; 183; 184) (including La and Cu NMR and NQR) provided evidence for local magnetic order near  $x = 1/8$  in  $\text{La}_{2-x}\text{Sr}_x\text{CuO}_4$  and  $\text{La}_{2-x}\text{Ba}_x\text{CuO}_4$ .

The work by Imai’s group(185) suggesting that local stripe order in variants of  $\text{La}_{2-x}\text{Sr}_x\text{CuO}_4$  could be detected through the “wipeout effect” of Cu NQR has motivated a considerable number of further studies using Cu and La NMR and NQR.(186; 187; 188; 189; 190; 191; 192; 193; 194; 195) Although there has been some con-

troversy over details of the interpretation (and in certain cases, there may be differences between samples), it is now generally agreed that NQR and NMR are sensitive to the onset of slow spin fluctuations whose appearance tends to correlate with the onset of local charge stripe pinning as determined by diffraction. In particular, the glassy nature of the ordering has been investigated. In the case of Eu-doped  $\text{La}_{2-x}\text{Sr}_x\text{CuO}_4$ , related information has been obtained by electron-spin resonance detected from a very low density of Gd impurities.(196; 197) A recent Cu NQR and Y NMR study(198) has shown that similar signatures are observed in Ca-doped  $\text{YBa}_2\text{Cu}_3\text{O}_6$ , consistent with the  $\mu\text{SR}$  study of Niedermayer *et al.*,(87) and suggestive of the presence of pinned stripes in that system at low temperatures. Direct evidence for local spatial inhomogeneities in  $\text{La}_{2-x}\text{Sr}_x\text{CuO}_4$  has been obtained from studies of NMR line broadening (199) and frequency-dependent NQR relaxation rates (200)

Several recent NMR studies(201; 202; 203; 204) have exploited the magnetic-field dependence of the technique to probe the spatial variation of nuclear spin-lattice relaxation rates in the vortex lattice state of cuprate superconductors. Vortex cores are region of suppressed superconductivity, so if there is a competing spin-stripe ordered phase, it will be enhanced and pinned(55; 56) in the neighborhood of the vortex core. Indeed,  $^{17}\text{O}$  NMR measurements on  $\text{YBa}_2\text{Cu}_3\text{O}_{6+y}$  and  $\text{YBa}_2\text{Cu}_4\text{O}_8$  indicate antiferromagnetic-like spin fluctuations and a reduced density of states associated with the vortex cores.(203; 204) (Similar results, along with evidence of static spin ordering in the vortex cores at low temperatures, have been reported(205) in  $\text{Tl}_2\text{Ba}_2\text{CuO}_{6+\delta}$ .) A  $\mu\text{SR}$  study of the details of the magnetic-field distribution in  $\text{YBa}_2\text{Cu}_3\text{O}_{6.50}$  suggests the presence of a small local hyperfine field near vortex cores.(206) For completeness, we note that while one neutron scattering study has indicated very weak, field-induced, elastic antiferromagnetic scattering in superconducting  $\text{YBa}_2\text{Cu}_3\text{O}_{6+y}$ ,(207) two other studies, focusing on the effect of a magnetic field on inelastic scattering, found no low frequency enhancement.(208; 209)

It has been demonstrated that stripe order has an impact on phonon heat transport.(210) The thermal conductivity increases slightly on cooling through the charge-ordering transition, exhibiting a normal peak at  $\sim 25$  K. The suppression of the latter peak in superconducting  $\text{La}_{2-x}\text{Sr}_x\text{CuO}_4$  has been attributed to the scattering of phonons by fluctuating stripes.(211) The doping dependence of the thermal conductivity measured in  $\text{YBa}_2\text{Cu}_3\text{O}_{6+y}$  and in mercury-cuprates has been interpreted as evidence for a 1/8 anomaly in those materials.(212) An enhancement of the thermal conductivity in  $\text{La}_{1.88}\text{Ba}_{0.12}\text{CuO}_4$  was originally noted by Sera *et al.*(213)

Indirect evidence of some form of local charge order can also be gleaned from the response of a system to electro-magnetic radiation(214). For instance, Raman scattering(215) was recently used to reveal charge or-

dering, and more importantly (for present purposes) to detect the effect of collective CDW motion at higher temperatures in  $\text{Sr}_{12}\text{Cu}_{24}\text{O}_{41}$ , a ladder system with a local electronic structure very similar to that of the cuprate superconductors. Careful measurements of the optical response of optimally doped  $\text{YBa}_2\text{Cu}_3\text{O}_{6+y}$  have revealed(216; 217) infrared active phonons with oscillator strength comparable to those in the undoped insulating compound. This has been plausibly interpreted as giving evidence of “fluctuating charge inhomogeneities” in the copper-oxide planes - the point being that for the phonons to be unscreened at that frequency, their local environment on some scale must be insulating.

ARPES experiments can also be interpreted as giving indirect evidence of local stripe order. At an empirical level, this can be done by looking(218; 219) at the evolution of the ARPES spectra in a sequence of materials in the  $\text{La}_2\text{CuO}_4$  family in which various types of stripe order have been detected; this provides a basis for identifying similar features in the ARPES spectrum of materials in which stripe order has not been established. For instance, stripe long-range order produces a tendency for the Fermi surface in the antinodal region of the Brillouin zone to be flat (one-dimensional), and to suppress spectral weight in the nodal region. Some of these same features, especially the differing impact on the nodal and antinodal regions, are induced by Zn doping of  $\text{Bi}_2\text{Sr}_2\text{CaCu}_2\text{O}_{8+\delta}$ , as well - plausibly reflecting(220) the tendency of Zn to pin local stripe order. More broadly, many of the most striking features of the observed(134; 138; 141; 221; 222) ARPES spectra can be naturally interpreted in terms of an underlying quasi one-dimensional electronic structure(20). Examples of this are the disappearance of the the coherent quasi-particle peak(223) upon heating above  $T_c$ , the dichotomy between the widths of the peaks as a function of momentum and energy in the normal state spectrum(129; 131), and the general structure of the spectra and the evolution of the Fermi surface with doping.(224; 225; 226; 227; 228; 229)

Finally, several probes have been used to search for the inhomogeneous distribution of bond-lengths expected from the lattice response to local charge stripe order. Pair-distribution-function (PDF) analysis of scattering data and extended X-ray absorption fine structure (EX-AFS) spectroscopy can detect instantaneous distributions of nearest-neighbor bond lengths. Both techniques have the potential to provide indirect evidence of dynamical, as well as static, stripes; however, whether they have sufficient sensitivity to detect the very small bond-length variations associated with charge modulation in the cuprates remains a topic of some contention. Božin *et al.*(230) reported a doping-dependent broadening of the in-plane Cu-O bond-length distribution in  $\text{La}_{2-x}\text{Sr}_x\text{CuO}_4$  detected by PDF analysis of neutron powder diffraction data. While the reported doping dependence is intriguing, the maximum enhancement of the bond-length spread is much too large to be compatible with the Debye-Waller factors measured

in a single-crystal neutron diffraction experiment on  $\text{La}_{1.85}\text{Sr}_{0.15}\text{CuO}_4$  by Braden *et al.*(231) A much more extreme discrepancy occurs with the EXAFS studies of  $\text{La}_{2-x}\text{Sr}_x\text{CuO}_4$  (and other cuprates) by Bianconi's group.(232; 233; 234) They report a low-temperature splitting of the in-plane Cu-O bond lengths of  $0.08 \text{ \AA}$ , which is not only incompatible with a large number of diffraction studies, but is also inconsistent with EXAFS analysis performed by other groups.(235; 236) Large atomic mean-square displacements detected in  $\text{YBa}_2\text{Cu}_3\text{O}_{6+y}$  by ion channeling(237) have been attributed to transitions associated with dynamic stripes, but the magnitude of the displacements and the temperature dependence are difficult to reconcile with other experiments.

In short, these various local measures of the distribution of lattice displacements are, in principle, a very good way to look for local charge-ordering tendencies, but it is important to reconcile the results obtained with different techniques. Where apparent inconsistencies exist, they must be resolved before unambiguous inferences can be made.

## VI. CONCLUSIONS

There are many reasons why identifying and studying fluctuations associated with the presence of "nearby" ordered states has become one of the main thrusts in the study of cuprate superconductors and related materials. To some extent, these states are interesting just because they occur somewhere in the (multidimensional) phase diagram of these intriguing materials. Quantum critical points associated with some of these orders have been proposed to be the explanation of the notoriously peculiar high-temperature ("normal state") behavior observed in many experiments. The possibility that certain local orders are inextricably linked with the phenomenon of high-temperature superconductivity is the most enticing reason of all. However, before we can determine whether a particular form of local order, such as local stripe order, could possibly be central to the problem of high temperature superconductivity, we need to determine whether or not it is ubiquitous in the families of materials which exhibit high-temperature superconductivity. Regardless of one's motivation, it is clear that the ability to identify the proximity to an ordered phase by the signatures of "fluctuating order" is very useful. This paper has focused on practical considerations pertinent to this task.

A combination of rather general scaling considerations concerning quantum critical phenomena, and specific insights gleaned from the solvable models studied, has lead us to articulate a number of "lessons" concerning the optimal way of obtaining information about nearby ordered states from experiment. **1)** The information is best obtained from the low-frequency part of the dynamic structure factor, preferably integrated over a small, but

non-zero range of frequencies, with the scale of frequencies set by the characteristic frequency of quantum fluctuations,  $E_G/\hbar$ . **2)** Weak disorder can make it easier, especially for static probes, to image the local order, as it can pin the fluctuations without greatly disrupting the intrinsic correlations. **3)** Dispersing features give information about the elementary excitations of the system; however, distinguishing dispersing features that arise from well defined quasi-particles characteristic of a well ordered or entirely disordered phase, from the multi-particle continua characteristic of quantum critical points can be exceedingly subtle. Specifically, even where one set of experiments can be sensibly interpreted in terms of band-structure effects, care must be taken in interpreting this as evidence of well defined electron-like quasiparticles. **4)** Several aspects of the  $E$  and  $\mathbf{k}$  dependence of the LDOS in the presence of weak disorder allow one, in principle, to distinguish interference effects from those of pinned incipient order. Interference effects in 2D produce peaks along *curves* in  $\mathbf{k}$  space which disperse as a function of energy in a manner which is directly related to the quasi-particle dispersion relations, such as could be measured in ARPES, and they may (or may not) have a strongly energy dependent phase. Pinning of incipient order produces peaks at well defined points in  $\mathbf{k}$  space which depend only weakly if at all on energy, and generally have an energy independent phase. **5)** It will often be true that interference effects and collective pinning will jointly produce complicated  $\mathbf{k}$  and  $E$  dependent properties that arise from a combination of both effects, especially in energy ranges in which both the dispersing and non-dispersing features lie at nearby values of  $\mathbf{k}$ .

In Section IV of this paper, we applied these ideas to an analysis of the evidence of local stripe order in a number of neutron scattering and STM measurements on various cuprate superconductors. The evidence of both spin- and charge-stripe order is unambiguous in the  $\text{La}_2\text{CuO}_4$  family of high-temperature superconductors. However, there is increasingly strong evidence of substantial local charge-stripe order, and probably nematic order as well, in  $\text{Bi}_2\text{Sr}_2\text{CaCu}_2\text{O}_{8+\delta}$  and  $\text{YBa}_2\text{Cu}_3\text{O}_{6+y}$ .

## VII. ACKNOWLEDGMENTS

We would like to dedicate this paper to our friend and collaborator, Victor J. Emery, whose untimely death we mourn. Many of the ideas discussed in this paper have been strongly influenced by Vic's seminal contributions to this field. We thank K. B. Cooper, S. L. Cooper, J.C.Davis, J. P. Eisenstein, J.Hoffman, P. Johnson, D-H.Lee, P.B.Littlewood, A. Polkovnikov, S.Sachdev, D.J.Scalapino, Z-X. Shen, A. Yazdani, and X. Zhou for useful and stimulating discussions. This work was supported in part by the National Science Foundation through the grants No. DMR 01-10329 (SAK at UCLA), DMR 01-32990 (EF, at the University of Illinois), DMR 99-78074 (VO, at Princeton University), by the David

and Lucille Packard Foundation (VO, at Princeton University), and (AK and CH at Stanford), and by the Department of Energy's Office of Science under contracts No. DE-AC02-98CH10886 (JMT, at Brookhaven National Laboratory), DE-FG03-01ER45929-A000 (AK and CH at Stanford University), and DE-FG03-00ER45798 (IPB at UCLA).

### Note Added:

After this work was completed, we received an advanced copy of a review article by S. Sachdev(238) which has overlapping material with the present paper, and reaches similar conclusions effects of incipient stripe order on the STM spectra.

### References

- [1] For brief reviews of the current evidence on various types of stripe order in the cuprates, see Refs. (2; 3; 4).
- [2] V. J. Emery, S. A. Kivelson, and J. Tranquada, Proc. Natl. Acad. Sci. **96**, 8814 (1999) and references therein.
- [3] J. Zaanen, *Nature*, **404**, 714 (2000).
- [4] S. Sachdev cond-mat/0203363, to be published in Proceedings of the Mexican Meeting on Mathematical and Experimental Physics, Mexico City, September 2001, Academic/Plenum Press.
- [5] S. A. Kivelson, E. Fradkin, and V. J. Emery, *Nature*, **393**, 550–553 (1998).
- [6] Fluctuations associated with off-diagonal, *i.e.* superconducting order, are best studied using different probes; see, for example, Refs. (7; 8; 9; 10; 11).
- [7] Z. A. Xu, N. Ong, Y. Wang, T. Kakeshita, and S. Uchida, *Nature*, **406**, 486–488 (2000).
- [8] Y. Wang, Z. A. Xu, T. Kakeshita, S. Uchida, S. Ono, Y. Ando, and N. P. Ong,  $\text{La}_{2-x}\text{Sr}_x\text{CuO}_4$  and *Phys. Rev. B*, **64**, 224519–224528 (2001);
- [9] I. Ussishkin, S. L. Sondhi, , and D. A. Huse, cond-mat/0204484
- [10] E. W. Carlson, S. A. Kivelson, V. J. Emery, and E. Manousakis, *Phys. Rev. Lett.*, **83**, 612 (2000).
- [11] I. Iguchi, T. Yamaguchi, and A. Sugimoto, *Nature*, **412**, 420–23 (2001).
- [12] For reviews of neutron and X ray evidence of stripes, see Ref. (13; 14)
- [13] J. M. Tranquada, *Neutron Scattering in Layered Copper-Oxide Superconductors*, edited by A. Furrer (Kluwer, Dordrecht, The Netherlands, 1998), pp. 225–260.
- [14] J. M. Tranquada, *AIP-Conference-Proceedings*, **483**, 336–340 (1999).
- [15] Recent reviews of the mechanisms of stripe formation in the cuprates and, more generally in doped antiferromagnets, often with rather different perspectives on the issue, can be found in Refs. (2; 16; 17; 18; 19; 20; 21; 22; 23).
- [16] J. Zaanen, *Journal of the Physics and Chemistry of Solids*, **59**, 1769 (1998).
- [17] M. Vojta and S. Sachdev, *Phys. Rev. Lett.* **83**, 3916 (1999).
- [18] S.R.White and D.J.Scalapino, *Phys. Rev. B* **61**, 6320 (2000).
- [19] S.R.White, I.Affleck, and D.J.Scalapino, *Phys. Rev. B* **65**, 165122 (2002).
- [20] E. W. Carlson, V. J. Emery, S. A. Kivelson, and D. Orgad, “Concepts in High Temperature Superconductivity” cond-mat/0206217, to be published in “The Physics of Conventional and Unconventional Superconductors” ed. by K. H. Bennemann and J. B. Ketterson (Springer-Verlag).
- [21] J.Zaanen and P. B. Littlewood, *Physical Review B* **50**, 7222 (1994).
- [22] M.Ichioka and K.Machida, *Journal of the Physical Society of Japan*, **68**, 4020 (1999).
- [23] N. Hasselmann, A.H.Castro Neto, C.M.Smith, *Phys. Rev. B* **65**, 220511 (2002).
- [24] Various perspectives concerning the relevance of local stripe order to other properties of the high temperature superconductors are reviewed in (20; 25; 26; 27).
- [25] J.Zaanen, O.Y.Osman, H.V.Kruis, Z.Nussinov, J.Tworzydlo, *Philosophical Magazine* **B81** 1485-531 (2001).
- [26] J.Lorenzana, C.Castellani, C.Di Castro, *Phys. Rev. B* **64**, 235127 (2001) and *ibid* 235128 (2001).
- [27] A.Castro-Neto, *Phys. Rev. B* **64**, 104509 (2001).
- [28] Several recent discussions of the role of competing orders in determining the phase diagram of the high temperature superconductors are contained in (2; 3; 29; 30; 31; 32; 33).
- [29] S.Sachdev, *Science* **288**, 475 (2000).
- [30] J.Orenstein and A.J.Millis, *Science*, **288**, 468-74 (2000).
- [31] S. Chakravarty, R. B. Laughlin, D. K. Morr, and C. Nayak, *Phys. Rev. B* **64**, 094503 (2001).
- [32] C.M.Varma, *Phys. Rev. B* **55**, 14554 (1997).
- [33] S. A. Kivelson, G. Aeppli, and V. J. Emery, Proc. Natl. Accad. of Sci. **98**, 11903-11907 (2001).
- [34] Other reviews of the experimental evidence of the existence of stripe order in the cuprates include those in Refs. (1; 20; 28).
- [35] D. J. Derro, E. W. Hudson, K. M. Lang, S. H. Pan, J. C. Davis, J. T. Markert, and A. L. de Lozanne *Phys. Rev. Lett.* **88**, 097002 (2002).
- [36] D.J. Hornbaker, S.-J. Kahng, S. Misra, B.W. Smith, A.T. Johnson, E.J. Mele, D.E. Luzzi, and A. Yazdani, *Science* **295**, 828 (2002). T.W. Odom, Jin-Lin Huang, and C.M. Lieber, *Journal of Physics-Condensed Matter* **14**, 18 (2002).
- [37] J. E. Hoffman, E.W. Hudson, K. M. Lang, V. Madhavan, S.H. Pan, H. Eisaki, S. Uchida, and J.C. Davis, *Science* **297**, 1148 (2002).
- [38] J. E. Hoffman, E. W. Hudson, K. M. Lang, V. Madhavan, H. Eisaki, S. Uchida, and J. C. Davis, *Science* **295**, 466 (2002).
- [39] C. Howald, H. Eisaki, N. Kaneko, and A. Kapitulnik, cond-mat/0201546.
- [40] One can also imagine “orbital stripes” which involve a unidirectional modulation of a staggered flux or d-density wave order.(41)
- [41] U.Schollwoeck, Sudip Chakravarty, J. O. Fjaerestad, J. B. Marston, M. Troyer, “Broken time-reversal symmetry in strongly correlated ladder structures”, cond-mat/0209444.
- [42] O. Zachar, S. A. Kivelson, and V. J. Emery, *Phys. Rev. B*, **57**, 1422 (1998).

[43] A nematic spin nematic is most easily pictured as a state in which the spin up and spin down electrons each form a nematic state, with their principle axes at  $90^\circ$  to each other.

[44] For extremely clear reviews, see S. Sachdev, *Science*, **288**, 475 (2000) and *Quantum Phase Transitions* (Cambridge University Press, Cambridge, UK) (1999), as well as (45).

[45] S. L. Sondhi, S. M. Girvin, J. P. Carini and D. Shahar, *Rev. Mod. Phys.* **69**, 315 (1997).

[46] The value of  $z$  can depend on many things, such as the character of a fermionic particle-hole continuum to which the order parameter couples; under many circumstances,  $z$  is either 1 or 2.  $\nu$  depends on the effective dimension,  $D+z$  and, to a lesser extent, on the symmetry of the order parameter; typically, for  $D \geq 2$ ,  $\nu$  is in the range  $2/3 \geq \nu \geq 1/2$ .

[47] In the presence of zero temperature dissipation, the system may be gapless, in which case the interpretation of  $\tau$  is more subtle. For simplicity, we ignore this possibility in the present paper, although it may well be much more general than was previously appreciated.(48)

[48] For a recent perspective on this issue, see A. Kapitulnik, N. Mason, S. A. Kivelson, and S. Chakravarty, *Phys. Rev. B*, **63**, 125322 (2001).

[49] The naive argument, which is often made, that at frequencies larger than  $E_G$  the quantum disordered phase looks like the ordered phase is thus not completely correct. There is, however, a more nearly correct version of this statement: at high frequencies, on both the ordered and disordered sides of the quantum critical point, the system looks quantum critical, and so looks the same whichever state is being probed.

[50] R. B. Griffiths, *Phys. Rev. Lett.* **23**, 17 (1969); B. McCoy and T. T. Wu, *Phys. Rev.* **176**, 631 (1968); D. C. Fisher, *Phys. Rev. Lett.* **69**, 534 (1992).

[51] A first order transition of this sort has been reported in the BEDT system by Lefebvre *et al*(52) and in (TMTSF)<sub>2</sub>PF<sub>6</sub> by Brown *et al*(53).

[52] S. Lefebvre, *et al* *Phys. Rev. Lett.* **85**, 5420-3 (2000).

[53] W. Yu, F. Zamborszky, B. Alavi, and S. E. Brown, “Inhomogeneous carrier density and the role of disorder in the normal state of (TMTSF)<sub>2</sub>PF<sub>6</sub>,” *Syn. Metals* (in press).

[54] The effect of the magnetic field on the competition between stripe and superconducting order has recently been extensively studied; see, for instance, Refs. (55; 56) and references therein. For an earlier related discussion, see (58).

[55] E. Demler, S. Sachdev, Y. Zhang, *Phys. Rev. Lett.* **87**, 067202 (2001); Y. Zhang, E. Demler, and S. Sachdev, cond-mat/0112343.

[56] S. A. Kivelson, D.-H. Lee, E. Fradkin and V. Oganesyan, to appear in *Phys. Rev. B*(2002), cond-mat/0205228.

[57] D. A. Ivanov, P. A. Lee and Xiao-Gang Wen, *Phys. Rev. Lett.* **84**, 3958 (2000).

[58] S.-C. Zhang, *Science* **275**, 1089 (1997); D. P. Arovas, A. J. Berlinsky, C. Kallin, and S.-C. Zhang *Phys. Rev. Lett.* **79**, 2871-2874 (1997).

[59] V. J. Emery and S. A. Kivelson, *Physica* **C209**, 597 (1993).

[60] O. Zachar, *Phys. Rev. B* **62**, 13836

[61] I. P. Bindloss, S. A. Kivelson, E. Fradkin, and V. Oganesyan, work in progress.

[62] For reviews of the the theory of the 1DEG, see Refs. (63; 64).

[63] V. J. Emery, *Theory of the one-dimensional electron gas*, in *Highly Conducting One-Dimensional Solids*, edited by J. T. Devreese, R. P. Evrard, and V. E. van Doren, 327 (Plenum, New York) (1979). More recent reviews can be found in E. Fradkin, *Field Theories of Condensed Matter Systems* (Addison-Wesley, Massachusetts) (1991).

[64] A. O. Gogolin, A. A. Nersesyan, and A. M. Tsvelik, *Bosonization and Strongly Correlated Systems* (Cambridge University Press, Cambridge) (1998).

[65] C. Kane and M. P. A. Fisher, *Phys. Rev. B* **68**, 1220 (1992); *ibid.* **72**, 724 (1994).

[66] S. Eggert, *Phys. Rev. Lett.* **84**, 4413 (2000); see also S. Eggert, H. Johannesson and A. Mattsson, *Phys. Rev. Lett.* **76**, 1505 (1996) and A. Mattsson, S. Eggert and H. Johannesson, *Phys. Rev. B* **56**, 15615 (1997).

[67] In practice, the distinction between curves along which  $N(\vec{k}, E)$ , indicative of quasiparticle interference effects, and peaks at isolated “ordering” vectors,  $\vec{k} = \vec{Q}$ , may not always be straightforward to establish in experiment. Consider the case in which there is an anisotropy of strength  $\alpha$  in the effective mass of the 2DEG, *i. e.*  $\epsilon_{\vec{k}} = \hbar^2(k_x^2 + \alpha k_y^2)/2m$ . In the limit of large anisotropy,  $\alpha \gg 1$ , when the effects of the finite  $\vec{k}$  resolution of actual experiments are taken into account, apparent peak-like structures can emerge. If we represent the effect of finite resolution by integrating the expression in Eq.4.1 over a range of momenta around different points along the ellipse  $\epsilon_{\vec{k}} = 4E$ , the integrated expression is peaked near  $\vec{k} = \pm 2\sqrt{2mE} \hat{e}_x$ , where it is a factor of  $\sqrt{\alpha}$  larger than where it is minimal near  $\sqrt{\alpha} \vec{k} = \pm 2\sqrt{2mE} \hat{e}_y$ . This sort of effect was invoked in Refs. (38) and (68) to explain dispersing peaks observed in STM on BSCCO.

[68] Qiang-Hua Wang and Dung-Hai Lee, “Quasiparticle Scattering Interference in High Temperature Superconductors” cond-mat/0205118.

[69] B. G. Briner, Ph. Hofmann, M. Doering, H.-P. Rust, E. W. Plummer, and A. M. Bradshaw, *Phys. Rev. B* **58**, 13931 (1998); P.T. Sprunger, L. Petersen, E.W. Plummer, E. Laegsgaard, and F. Besenbacher, *Science* **275**, 1764 (1997).

[70] D. Podolsky, E. Demler, K. Damle, and B.I.Halperin, “Translational Symmetry Breaking in the Superconducting States of the Cuprates: Analysis of the Quasi-Particle Density of States,” cond-mat/0204011.

[71] J. M. Byers, M.E.Flatté, and D.J.Scalapino, *Phys. Rev. Lett.* **71**, 3363 (1993).

[72] A. Polkovnikov, M. Vojta, and S. Sachdev, *Phys. Rev. B* **65**, 220509 (2002).

[73] S. Ono, Y. Ando, T.Murayama, F. E. Balakirev, J. B. Betts, and G. S. Boebinger, *Phys. Rev. Lett.* **85**, 638 (2000); A.W.Tyler, Y.Ando, F.F.Balakirev, A.Passner, G.S.Boebinger, A.J.Schofield, A.P.Mackenzie, and O.Laborde, *Review B (Condensed Matter)*, vol. *Phys. Rev. B* **57**, 728 (1998). Y. Ando, G.S.Boebinger, A. Passner, N.L.Wang, C. Geibel, F.Steglich, I.E.Trofimov, and F.F.Balakirev, *Phys. Rev. B* **56**, 8530 (1997).

[74] S. Katano, M. Sato, K. Yamada, T. Suzuki, and T. Fukase, *Phys. Rev. B* **62**, R14677 (2000).

[75] B. Lake, H. M. Rønnow, N. B. Christensen, G. Aeppli, K. Lefmann, D. F. McMorrow, P. Vorderwisch,

P. Smeibidl, N. Mangkorntong, T. Sasagawa, et al., *Nature* **415**, 299 (2002).

[76] B. Lake, G. Aeppli, K.N. Clausen, D.F. McMorrow, K. Lefmann, N.E. Hussey, N. Mangkorntong, M. Mohara, H. Takagi, T.E. Mason, and A. Schröder, *Science* **291**, 1759 (2001).

[77] B. Khaykovich, Y. S. Lee, R. W. Erwin, S.-H. Lee, S. Wakimoto, K. J. Thomas, M. A. Kastner, and R. J. Birgeneau, *Phys. Rev. B* **66**, 014528 (2002).

[78] Y. Ando, *Stripes and Charge Transport Properties of High- $T_c$  Cuprates*, ICTP Workshop on Intrinsic Multiscale Structure and Dynamics in Complex Electronic Oxides, Trieste, July 2002. (To be published in the Proceedings of the ICTP Workshop as a World Scientific book.), cond-mat/0206332.

[79] M. P. Lilly, K. B. Cooper, J. P. Eisenstein, L. N. Pfeiffer, and K. W. West, *Phys. Rev. Lett.* **82**, 394 (1999); R. R. Du, D. C. Tsui, H. L. Stormer, L. N. Pfeiffer, K. W. Baldwin KW, and K. W. West, *Solid State Comm.* **109**, 389 (1999).

[80] Y. Ando, K. Segawa, S. Komiya, and A. N. Lavrov, *Phys. Rev. Lett.* **88**, 137005 (2002).

[81] J. M. Tranquada, J. D. Axe, N. Ichikawa, A. R. Moodenbaugh, Y. Nakamura, and S. Uchida, *Phys. Rev. Lett.* **78**, 338 (1997).

[82] N. Ichikawa, S. Uchida, J. M. Tranquada, T. Niemöller, P. M. Gehring, S.-H. Lee, and J. R. Schneider, *Phys. Rev. Lett.* **85**, 1738 (2000).

[83] S. Wakimoto, J. M. Tranquada, T. Ono, K. M. Kojima, S. Uchida, S.-H. Lee, P. M. Gehring, and R. J. Birgeneau, *Phys. Rev. B* **64**, 174505 (2001).

[84] M. Fujita, H. Goka, K. Yamada, and M. Matsuda, *Phys. Rev. Lett.* **88**, 167008 (2002).

[85] T. Suzuki, T. Goto, K. Chiba, T. Shinoda, T. Fukase, H. Kimura, K. Yamada, M. Ohashi, and Y. Yamaguchi, *Phys. Rev. B* **57**, R3229 (1998).

[86] H. Kimura, K. Hirota, H. Matsushita, K. Yamada, Y. Endoh, S.-H. Lee, C. F. Majkrzak, R. Erwin, G. Shirane, M. Greven, et al., *Phys. Rev. B* **59**, 6517 (1999).

[87] C. Niedermayer, C. Bernhard, T. Blasius, A. Golnik, A. Moodenbaugh, and J. I. Budnick, *Phys. Rev. Lett.* **80**, 3843 (1998).

[88] S. Wakimoto, G. Shirane, Y. Endoh, K. Hirota, S. Ueki, K. Yamada, R. J. Birgeneau, M. A. Kastner, Y. S. Lee, P. M. Gehring, et al., *Phys. Rev. B* **60**, R769 (1999).

[89] M. Matsuda, Y. S. Lee, M. Greven, M. A. Kastner, R. J. Birgeneau, K. Yamada, Y. Endoh, P. Böni, S.-H. Lee, S. Wakimoto, et al., *Phys. Rev. B* **61**, 4326 (2000).

[90] Y. S. Lee, R. J. Birgeneau, M. A. Kastner, Y. Endoh, S. Wakimoto, K. Yamada, R. W. Erwin, S.-H. Lee, and G. Shirane, *Phys. Rev. B* **60**, 3643 (1999).

[91] H. A. Mook, P. Dai, and F. Doğan, *Phys. Rev. Lett.* **88**, 097004 (2002).

[92] H. A. Mook, private communication.

[93] J. M. Tranquada, in *Neutron Scattering in Layered Copper-Oxide Superconductors*, edited by A. Furrer (Kluwer, Dordrecht, The Netherlands, 1998), p. 225.

[94] S.-H. Lee and S.-W. Cheong, *Phys. Rev. Lett.* **79**, 2514 (1997).

[95] H. Yoshizawa, T. Kakeshita, R. Kajimoto, T. Tanabe, T. Katsufuji, and Y. Tokura, *Phys. Rev. B* **61**, R854 (2000).

[96] R. Kajimoto, K. Ishizaka, H. Yoshizawa, and Y. Tokura, eprint cond-mat/0202288.

[97] P. G. Radaelli, D. E. Cox, L. Capogna, S.-W. Cheong, and M. Marezio, *Phys. Rev. B* **59**, 14440 (1999).

[98] R. Wang, J. Gui, Y. Zhu, and A. R. Moodenbaugh, *Phys. Rev. B* **61**, 11946 (2000).

[99] S. Mori, C. H. Chen, and S.-W. Cheong, *Nature* **392**, 473 (1998).

[100] S. Mori, C. H. Chen, and S.-W. Cheong, *Phys. Rev. Lett.* **81**, 3972 (1998).

[101] J. M. Tranquada, N. Ichikawa, and S. Uchida, *Phys. Rev. B* **59**, 14712 (1999).

[102] T. R. Thurston, R. J. Birgeneau, M. A. Kastner, N. W. Preyer, G. Shirane, Y. Fujii, K. Yamada, Y. Endoh, K. Kakurai, M. Matsuda, et al., *Phys. Rev. B* **40**, 4585 (1989).

[103] S.-W. Cheong, G. Aeppli, T. E. Mason, H. Mook, S. M. Hayden, P. C. Canfield, Z. Fisk, K. N. Clausen, and J. L. Martinez, *Phys. Rev. Lett.* **67**, 1791 (1991).

[104] T. R. Thurston, P. M. Gehring, G. Shirane, R. J. Birgeneau, M. A. Kastner, Y. Endoh, M. Matsuda, K. Yamada, H. Kojima, and I. Tanaka, *Phys. Rev. B* **46**, 9128 (1992).

[105] J. M. Tranquada, B. J. Sternlieb, J. D. Axe, Y. Nakamura, and S. Uchida, *Nature* **375**, 561 (1995).

[106] K. Yamada, S. Wakimoto, G. Shirane, C. H. Lee, M. A. Kastner, S. Hosoya, M. Greven, Y. Endoh, and R. J. Birgeneau, *Phys. Rev. Lett.* **75**, 1626 (1995).

[107] This interpretation is further supported by the finding that the magnetic  $S(\vec{k}, \omega)$  in near optimally doped  $\text{La}_{2-x}\text{Sr}_x\text{CuO}_4$  has scaling properties consistent with its being dominated by a nearby stripe ordering quantum critical point; see G. Aeppli, T. E. Mason, S. M. Hayden, H. A. Mook, and J. Kulda, *Science* **278**, 1432 (1997).

[108] M. Matsuda, R. J. Birgeneau, H. Chou, Y. Endoh, M. A. Kastner, H. Kojima, K. Kuroda, G. Shirane, I. Tanaka, and K. Yamada, *J. Phys. Soc. Japan* **62**, 443 (1993).

[109] K. Hirota, K. Yamada, I. Tanaka, and H. Kojima, *Physica B* **241–243**, 817 (1998).

[110] J. M. Tranquada, N. Ichikawa, K. Kakurai, and S. Uchida, *J. Phys. Chem. Solids* **60**, 1019 (1999).

[111] It is certain that one effect of the Zn impurities is to pin the charge stripe fluctuations. It may also be that the missing Cu spin plays an important role in slowing the spin-fluctuations in the neighborhood of the Zn - the potential importance of this form of coupling, based on the behavior of a Kondo impurity in a system close to a magnetic quantum critical point, has been stressed in Ref. (112).

[112] S. Sachdev, C. Buragohain and M. Vojta, *Science*, **286**, 2479 (1999).

[113] K. Hirota, *Physica C* **357-360**, 61 (2001).

[114] K. Yamada, C. H. Lee, K. Kurahashi, J. Wada, S. Wakimoto, S. Ueki, Y. Kimura, Y. Endoh, S. Hosoya, G. Shirane, et al., *Phys. Rev. B* **57**, 6165 (1998).

[115] Han-Dong Chen, Jiang-Ping Hu, Sylvain Capponi, Enrico Arrigoni and Shou-Cheng Zhang, *Phys. Rev. Lett.* **89**, 137004 (2002).

[116] U. Low, V.J. Emery, K. Fabricius, and S.A. Kivelson, *Phys. Rev. Lett.* **72**, 1918 (1994).

[117] Ali Yazdani, C.M. Howald, C.P. Lutz, A. Kapitulnik, and D.M. Eigler, *Phys. Rev. Lett.* **83**, 176 (1999).

[118] E.W. Hudson, S.H. Pan, A.K. Gupta, K.W. Ng, and J.C. Davis, *Science* **285**, 88 (1999).

[119] S.H. Pan, E.W. Hudson, K.M. Lang KM, H. Eisaki, S.

Uchida, and J.C. Davis *Nature*, **403**, 746 (2000).

[120] C. Howald, H. Eisaki, N. Kaneko, M. Greven, and A. Kapitulnik, preprint.

[121] S.H. Pan, J.P. O'Neal, R.L. Badzey, C. Chamon, H. Ding, J.R. Engelbrecht, Z. Wang, H. Eisaki, S. Uchida, A.K. Gupta, K.W. Ng, E.W. Hudson, K.M. Lang, and J.C. Davis, *Nature* **413**, 282 (2001).

[122] K.M. Lang, V. Madhavan, J. E. Hoffman, E.W. Hudson, H. Eisaki, S. Uchida, and J.C. Davis, *Nature* **415**, 412 (2002).

[123] S.H. Pan, E.W. Hudson, A.K. Gupta, K.-W. Ng, H. Eisaki, S. Uchida, and J.C. Davis, *Phys. Rev. Lett.* **85**, 1536 (2000).

[124] Ch. Renner, B. Revaz, K. Kadowaki, I. Maggio-Apprile, and O. Fischer, *Phys. Rev. Lett.* **80**, 3606 (1998).

[125] P.T. Sprunger, L. Petersen, E.W. Plummer, E. Laegsgaard, and F. Besenbacher, *Science* **275**, 1764 (1997).

[126] J. Friedel, *Nuovo Cimento Suppl.* **7**, 287 (1958).

[127] M.E. Crommie, C.P. Lutz, and D.M. Eigler, *Nature*, **363**, 524.

[128] Anatoli Polkovnikov, Subir Sachdev and Matthias Vojta, "Spin collective mode and quasiparticle contributions to STM spectra of d-wave superconductors with pinning", *Proceedings of LT 23*, Hiroshima (Japan, 2002), cond-mat/0208334.

[129] D. Orgad, E. Carlson, S. A. Kivelson, V. J. Emery, X. J. Zhou and Z-X. Shen, *Phys. Rev. Lett.* **86**, 4362 (2001).

[130] For technical reasons, what is actually plotted in Fig. 5 is  $\bar{N}^<(k) \equiv \lim_{T_K \rightarrow \infty} \int_{-\infty}^{\infty} dE f(E) N(k, E)$ , but the distinction between this and the quantity defined in the text is not important, here.

[131] G.-H. Gweon, J.D. Denlinger, J.W. Allen, R. Claessen, C.G. Olson, H. Hoechst, J. Marcus, C. Schlenker, and L.F. Schneemeyer, cond-mat/0103470.

[132] At very low energies and at low temperatures there is good reason to believe, and compelling evidence to confirm that the nodal quasiparticles in the superconducting state are well defined and long-lived. See Chiao May, R. W. Hill, C. Lupien, L. Taillefer, P. Lambert, R. Gagnon, and P. Fournier, *Phys. Rev. B* **62**, 3554 (2000). However, most of the dispersing features seen in STM are at higher energies, typically at energies on the order of  $\Delta_0/2$ , where even at low temperatures there is no evidence of well defined quasi-particles.

[133] M. Norman, M. Randeria, H. Ding and J. C. Campuzano, *Phys. Rev. B* **52**, 615 (1994).

[134] Andrea Damascelli, Zhi-Xun Shen and Zahid Hussain, "Angle-resolved photoemission spectroscopy of the cuprate superconductors", *Rev. Mod. Phys* in press, cond-mat/0208504.

[135] A. Polkovnikov, S. Sachdev, and M. Vojta, "Spin collective mode and quasiparticle contributions to STM spectra of d-wave superconductors with pinning," cond-mat/0208334.

[136] P. V. Bogdanov, A. Lanzara, S. A. Kellar, X. J. Zhou, E. D. Lu, W. J. Zheng, G. Gu, J.-I. Shimoyama, K. Kishio, H. Ikeda, R. Yoshizaki, Z. Hussain, and Z. X. Shen, *Phys. Rev. Lett.* **85**, 2581 (2000).

[137] A. Kaminski, M. Randeria, J. C. Campuzano, M. R. Norman, H. Fretwell, J. Mesot, T. Sato, T. Takahashi, and K. Kadowaki, *Phys. Rev. Lett.* **86**, 1070 (2001).

[138] T. Valla, A. V. Fedorov, P. D. Johnson, B. O. Wells, S. L. Hulbert, Q. Li, G. D. Gu, and N. Koshizuka, *Science* **285**, 2110 (1999).

[139] A.G. Loeser, Z.X. Shen, M.C. Schabel, C. Kim, M. Zhang, A. Kapitulnik, and P. Fournier, *Phys. Rev. B* **56**, 14185 (1997)

[140] H. Ding, J. C. Campuzano, A. F. Bellman, T. Yokoya, M. R. Norman, M. Randeria, T. Takahashi, H. Katayama-Yoshida, T. Mochiku, K. Kadowaki, and G. Jennings, *Phys. Rev. Lett.* **74**, 2784 (1995).

[141] A. V. Fedorov, T. Valla, P. D. Johnson, Q. Li, G. D. Gu, and N. Koshizuka, *Phys. Rev. Lett.* **82** (1999).

[142] C. H. Chen, S.-W. Cheong, and A. S. Cooper, *Phys. Rev. Lett.* **71**, 2461 (1993).

[143] J. Li, Y. Zhu, J. M. Tranquada, K. Yamada, and D. J. Buttrey, eprint cond-mat/0207398.

[144] E. Fradkin and S. A. Kivelson, *Phys. Rev. B* **59**, 8065 (1999); E. Fradkin, S. A. Kivelson, E. Manousakis and K. Nho, *Phys. Rev. Lett.* **84**, 1982 (2000).

[145] K. B. Cooper, M. P. Lilly, J. P. Eisenstein, L. N. Pfeiffer, and K. W. West, "The Onset of Anisotropic Transport of Two-Dimensional Electrons in High Landau Levels: An Isotropic-to-Nematic Liquid Crystal Phase Transition?", cond-mat/0203174.

[146] H. Fukuyama, P. Platzman and P. W. Anderson, *Phys. Rev. B* **19**, 5211 (1979); A. A. Koulakov, M. M. Fogler, and B. I. Shklovskii, *Phys. Rev. Lett.* **76**, 499 (1996); R. Moessner and J. T. Chalker, *Phys. Rev. B* **54**, 5006 (1996).

[147] K. B. Cooper, M. P. Lilly, J. P. Eisenstein, T. Jungwirth, L. N. Pfeiffer and K. W. West, *Solid State Commun.* **119**, 89 (2001); J. Zhu, W. Pan, H. L. Stormer, L. N. Pfeiffer and K. W. West, *Phys. Rev. Lett.* **88**, 116803 (2002).

[148] M. P. Lilly, K. B. Cooper, J. P. Eisenstein, L. N. Pfeiffer and K. W. West, *Phys. Rev. Lett.* **83**, 824 (1999); W. Pan, T. Jungwirth, H. L. Stormer, D. C. Tsui, A. H. MacDonald, S. M. Girvin, L. Smrcka, L. N. Pfeiffer, K. W. Baldwin and K. W. West, *Phys. Rev. Lett.* **85**, 3257 (2000).

[149] D. N. Basov, private communication.

[150] D. N. Basov *et al*, *Phys. Rev. Lett.* **74**, 598-601 (1995).

[151] T. Noda, H. Eisaki, and S. Uchida, *Science* **286**, 265 (1999).

[152] V. J. Emery, E. Fradkin, S. A. Kivelson, and T. C. Lubensky, *Phys. Rev. Lett.* **85**, 2160 (2000).

[153] P. Prelovšek, T. Tohyama, and S. Maekawa, *Phys. Rev. B* **64**, 052512 (2001).

[154] Y. Ando, A. N. Lavrov, and K. Segawa, *Phys. Rev. Lett.* **83**, 2813 (1999).

[155] A. Jánossy, F. Simon, and T. Fehér, *Phys. Rev. Lett.* **85**, 474 (2000).

[156] A. S. Moskvin and Y. D. Panov, *Solid State Commun.* **122**, 253 (2002).

[157] For a comprehensive discussion see P. G. de Gennes and J. Prost, *The Physics of Liquid Crystals* (Oxford Science Publications).

[158] M. Rübhausen, S. Yoon, S. L. Cooper, K. H. Kim, and S-W. Cheong, *Phys. Rev. B* **62**, R4782 (2000); S. Yoon, M. Rübhausen, S. L. Cooper, K. H. Kim, and S-W. Cheong *Phys. Rev. Lett.* **85**, 3297 (2000).

[159] H. A. Mook, P. Dai, F. Doğan, and R. D. Hunt, *Nature* **404**, 729 (2000).

[160] L. Pintschovius, W. Reichardt, M. Kläser, T. Wolf, and H. v. Löhneysen, *Phys. Rev. Lett.* **89**, 037001 (2002).

[161] J. M. Tranquada, K. Nakajima, M. Braden, L.

Pintschovius, and R. J. McQueeney, Phys. Rev. Lett. **88**, 075505 (2002).

[162] A. R. Moodenbaugh, Y. Xu, M. Suenaga, T. J. Folkerts, and R. N. Shelton, Phys. Rev. B **38**, 4596 (1988).

[163] M. K. Crawford, R. L. Harlow, E. M. McCarron, W. E. Farneth, J. D. Axe, H. Chou, and Q. Huang, Phys. Rev. B **44**, 7749 (1991).

[164] M. K. Crawford, W. E. Farneth, E. M. M. III, R. L. Harlow, and A. H. Moudden, Science **250**, 1390 (1990).

[165] G.-M. Zhao, M. B. Hunt, H. Keller, and K. A. Müller, Nature **385**, 236 (1997).

[166] C. Panagopoulos, J. L. Tallon, B. D. Rainford, T. Xiang, J. R. Cooper, and C. A. Scott, Phys. Rev. B **66**, 064501 (2002).

[167] J. Takeya, Y. Ando, S. Komiya, and X. F. Sun, Phys. Rev. Lett. **88**, 077001 (2002).

[168] Y. Koike, A. Kobayashi, T. Kawaguchi, M. Kato, T. Noji, Y. Ono, T. Hikita, and Y. Saito, Solid State Commun. **82**, 889 (1992).

[169] I. Watanabe, T. Adachi, K. Takahashi, S. Yairi, Y. Koike, K. Nagamine, and K. Nagamine, Phys. Rev. B **65**, 180516 (2002).

[170] J. L. Tallon, C. Bernhard, H. Shaked, R. L. Hitterman, and J. D. Jorgensen, Phys. Rev. B **51**, 12911 (1995).

[171] M. Akoshima and Y. Koike, J. Phys. Soc. Japan **67**, 3653 (1998).

[172] Y. Ando and K. Segawa, Phys. Rev. Lett. **88**, 167005 (2002).

[173] M. Akoshima, Y. Koike, I. Watanabe, and K. Nagamine, Phys. Rev. B **62**, 6761 (2000).

[174] I. Watanabe, M. Akoshima, Y. Koike, S. Ohira, and K. Nagamine, Phys. Rev. B **62**, 14524 (2000).

[175] W. L. Yang, H. H. Wen, and Z. X. Zhao, Phys. Rev. B **62**, 1361 (2000).

[176] Y. Ando, S. Ono, J. Takeya, X. F. Sun, J. B. Betts, and G. S. Boeginger, (unpublished).

[177] H.-H. Klauss, W. Wagener, M. Hillberg, W. Kopmann, H. Walf, F. J. Litterst, M. Hücker, and B. Büchner, Phys. Rev. Lett. **85**, 4590 (2000).

[178] B. Nachumi, Y. Fudamoto, A. Keren, K. M. Kojima, M. Larkin, G. M. Luke, J. Merrin, O. Tchernyshyov, Y. J. Uemura, N. Ichikawa, et al., Phys. Rev. B **58**, 8760 (1998).

[179] A. T. Savici, Y. Fudamoto, I. M. Gat, T. Ito, M. I. Larkin, Y. J. Uemura, G. M. Luke, K. M. Kojima, Y. S. Lee, M. A. Kastner, et al., Phys. Rev. B **66**, 014524 (2002).

[180] J. H. Cho, F. Borsa, D. C. Johnston, and D. R. Torgeson, Phys. Rev. B **46**, 3179 (1992).

[181] H. Tou, M. Matsumura, and H. Yamagata, J. Phys. Soc. Japan **62**, 1474 (1993).

[182] T. Goto, S. Kazama, K. Miyagawa, and T. Fukase, J. Phys. Soc. Japan **63**, 3494 (1994).

[183] S. Ohsugi, Y. Kitaoka, H. Yamanaka, K. Ishida, and K. Asayama, J. Phys. Soc. Japan **63**, 2057 (1994).

[184] T. Goto, K. Chiba, M. Mori, T. Suzuki, K. Seki, and T. Fukase, J. Phys. Soc. Japan **66**, 2870 (1997).

[185] A. W. Hunt, P. M. Singer, K. R. Thurber, and T. Imai, Phys. Rev. Lett. **82**, 4300 (1999).

[186] P. M. Singer, A. W. Hunt, A. F. Cederström, and T. Imai, Phys. Rev. B **60**, 15345 (1999).

[187] M.-H. Julien, F. Borsa, P. Carretta, M. Horvatić, C. Berthier, and C. T. Lin, Phys. Rev. Lett. **83**, 604 (1999).

[188] B. J. Suh, P. C. Hammel, M. Hücker, and B. Büchner, Phys. Rev. B **59**, R3952 (1999).

[189] B. J. Suh, P. C. Hammel, M. Hücker, B. Büchner, U. Ammerahl, and A. Revcolevschi, Phys. Rev. B **61**, R9265 (2000).

[190] N. J. Curro, P. C. Hammel, B. J. Suh, M. Hücker, B. Büchner, U. Ammerahl, and A. Revcolevschi, Phys. Rev. Lett. **85**, 642 (2000).

[191] G. B. Teitelbaum, B. Büchner, and H. de Gronckel, Phys. Rev. Lett. **84**, 2949 (2000).

[192] M.-H. Julien, A. Campana, A. Rigamonti, P. Carretta, F. Borsa, P. Kuhns, A. P. Reyes, W. G. Moulton, M. Horvatić, C. Berthier, et al., Phys. Rev. B **63**, 144508 (2001).

[193] A. W. Hunt, P. M. Singer, A. F. Cederström, and T. Imai, Phys. Rev. B **64**, 134525 (2001).

[194] G. B. Teitelbaum, I. M. Abu-Shiekah, O. Bakharev, H. B. Brom, and J. Zaanen, Phys. Rev. B **63**, 020507 (2001).

[195] B. Simović, P. C. Hammel, M. Hücker, B. Büchner, and A. Revcolevschi, cond-mat/0206497.

[196] V. Kataev, B. Rameev, B. Büchner, M. Hücker, and R. Borowski, Phys. Rev. B **55**, R3394 (1997).

[197] V. Kataev, B. Rameev, A. Validov, B. Büchner, M. Hücker, and R. Borowski, Phys. Rev. B **58**, R11 876 (1998).

[198] P. M. Singer and T. Imai, Phys. Rev. Lett. **88**, 187601 (2002).

[199] J. Haase, C. P. Slichter, R. Stern, C. T. Milling, and D. G. Hinks, Physica C **341-348**, 1727-30 (2000).

[200] P. M. Singer, A. W. Hunt, and T. Imai, Phys. Rev. Lett. **88**, 047602 (2002).

[201] N. J. Curro, C. Milling, J. Haase, and C. P. Slichter, Phys. Rev. B **62**, 3473 (2000).

[202] V. F. Mitrović, E. E. Sigmund, M. Eschrig, H. N. Bachman, W. P. Halperin, A. P. Reyes, P. Kuhns, and W. G. Moulton, Nature **413**, 501 (2001).

[203] V. F. Mitrović, E. E. Sigmund, W. P. Halperin, A. P. Reyes, P. Kuhns, and W. G. Moulton, eprint cond-mat/0202368.

[204] K. Kakuyanagi, K. Kumagai, and Y. Matsuda, Phys. Rev. B **65**, 060503 (2002).

[205] K. Kakuyanagi, K. Kumagai, Y. Matsuda, and M. Hasegawa, “Antiferromagnetic ordering and disappearance of pseudogap within the vortex core of  $Tl_2Ba_2CuO_{6+\delta}$ ,” cond-mat/0206362.

[206] R. I. Miller, R. F. Kiefl, J. H. Brewer, J. E. Sonier, J. Chakhalian, S. Dunsiger, G. D. Morris, A. N. Price, D. A. Bonn, W. H. Hardy, et al., Phys. Rev. Lett. **88**, 137002 (2002).

[207] D. Vaknin, J. L. Zarestky, and L. L. Miller, Physica C **329**, 109 (2000).

[208] P. Bourges, H. Casalta, L. P. Regnault, J. Bossy, P. Burlet, C. Vettier, E. Beaugnon, P. Gautier-Picard, and R. Tournier, Physica B **234-236**, 830 (1997).

[209] P. Dai, H. A. Mook, G. Aeppli, S. M. Hayden, and F. Doğan, Nature **406**, 965 (2000).

[210] C. Hess, B. Büchner, M. Hücker, R. Gross, and S.-W. Cheong, Phys. Rev. B **59**, R10 397 (1999).

[211] O. Baberski, A. Lang, O. Maldonado, M. Hücker, B. Büchner, and A. Freimuth, Europhys. Lett. **44**, 335 (1998).

[212] J. L. Cohn, C. P. Popoviciu, Q. M. Lin, and C. W. Chu, Phys. Rev. B **59**, 3823 (1999).

[213] M. Sera, S. Shamoto, M. Sato, I. Watanabe, S. Nakashima, and K. Kumagai, Solid State Commun. **74**, 951 (1990).

[214] For a discussion of the electromagnetic signatures of CDW order, see G. Grüner, "Density Waves in Solids," (Addison-Wesley, Reading, 1994).

[215] G. Blumberg, P. Littlewood, A. Gozar, B. S. Dennis, N. Motoyama, H. Eisaki, and S. Uchida, *Science* **297**, 584 (2002).

[216] C. C. Homes, A. W. McConnell, B. P. Clayman, D. A. Bonn, R. Liang, W. N. Hardy, M. Inoue, H. Negishi, P. Fournier, and R. L. Greene, *Phys. Rev. Lett.* **84**, 5391 (2000).

[217] C. Bernhard, T. Holden, J. Humlcek, D. Munzar, A. Golnik, M. Klser, Th. Wolf, L. Carr, C. Homes, B. Keimer, and M. Cardona Solid State Communications, **121**, 93 (2001).

[218] X. J. Zhou, P. Bogdanov, S. A. Kellar, T. Noda, H. Eisaki, S. Uchida, Z. Hussain, Z.-X. Shen, *Science* **286**, 268-72 (1999).

[219] Zhou, X.J.; Yoshida, T.; Kellar, S.A.; Bogdanov, P.V.; Lu, E.D.; Lanzara, A.; Nakamura, M.; Noda, T.; Kakeshita, T.; Eisaki, H.; Uchida, S.; Fujimori, A.; Hussain, Z.; Shen, Z.-X. *Phys. Rev. Lett.* **86**, 5578-81 (2001).

[220] P. J. White, Z. X. Shen, D. L. Feng, C. Kim, M. Z. Hasan, J. M. Harris, A. G. Loeser, H. Ikeda, R. Yoshizaki, G. D. Gu, and N. Koshizuka "Photoemission Studies on Bi<sub>2</sub>Sr<sub>2</sub>CaCuZnO - Electronic Structure Evolution and Temperature Dependence," cond-mat/9901349

[221] J. C. Campuzano, M. R. Norman, and M. Randeria, "Photoemission in the High T<sub>c</sub> Superconductors," cond-mat/0209476, to appear in "Physics of Conventional and Unconventional Superconductors", ed. K. H. Bennemann and J. B. Ketterson (Springer-Verlag).

[222] A. Ino, C. Kim, T. Mizokawa, Z.-X. Shen, A. Fujimori, M. Takaba, K. Tamasaku, H. Eisaki, and S. Uchida, *J. Phys. Soc. Jpn.* **68**, 1496 (1999).

[223] E. W. Carlson, D. Orgad, S. A. Kivelson, and V. J. Emery, *Phys. Rev. B* **62**, 3422 (2001).

[224] M. I. Salkola, V. J. Emery, and S. A. Kivelson, *Phys. Rev. Lett.* **77**, 155 (1996).

[225] M. Granath, V. Oganesyan, D. Orgad, and S. A. Kivelson, *Phys. Rev. B* **65**, 184501 (2002).

[226] M. Granath, V. Oganesyan, S. A. Kivelson, E. Fradkin, and V. J. Emery, *Phys. Rev. Lett.* **86**, 167011 (2001)

[227] M. G. Zachar, R. Eder, E. Arrigoni, and W. Hanke, *Phys. Rev. Lett.* **85**, 2585 (2000) and cond-mat/0103030.

[228] M. Ichioka and K. Machida, *J. Phys. Soc. Jan.* **68**, 4020 (1999).

[229] J. Eroles, G. Ortiz, A. V. Balatsky, and A. R. Bishop, *Phys. Rev. B* **64**, 174510 (2001).

[230] E. S. Božin, G. H. Kwei, H. Takagi, and S. J. L. Billinge, *Phys. Rev. Lett.* **84**, 5856 (2000).

[231] M. Braden, M. Meven, W. Reichardt, L. Pintschovius, M. T. Fernandez-Diaz, G. Heger, F. Nakamura, and T. Fujita, *Phys. Rev. B* **63**, 140510 (2001).

[232] A. Lanzara, N. L. Saini, T. Rossetti, A. Bianconi, H. Oyanagi, H. Yamaguchi, and Y. Maeno, *Solid State Commun.* **97**, 93 (1996).

[233] A. Bianconi, N. L. Saini, A. Lanzara, M. Missori, T. R. H. Oyanagi, H. Yamaguchi, K. Oka, and T. Ito, *Phys. Rev. Lett.* **76**, 3412 (1996).

[234] N. L. Saini, A. Lanzara, H. Oyanagi, H. Yamaguchi, K. Oka, T. Ito, and A. Bianconi, *Phys. Rev. B* **55**, 12759 (1997).

[235] T. Niemöller, B. Büchner, M. Cramm, C. Huhnt, L. Tröger, and M. Tischer, *Physica C* **299**, 191 (1998).

[236] D. Haskel, E. A. Stern, F. Dogan, and A. R. Moodenbaugh, *Phys. Rev. B* **61**, 7055 (2000).

[237] R. P. Sharma, S. B. Ogale, Z. H. Zhang, J. R. Liu, W. K. Chu, B. Veal, A. Paulikas, H. Zheng, and T. Venkatesan, *Nature* **404**, 736 (2000).

[238] S. Sachdev, "Order and quantum phase transitions in the cuprate superconductors," unpublished.